processes

MDPI

Article

Small-Scale Solids Production Plant with Cooling Crystallization, Washing, and Drying in a Modular, Continuous Plant

Stefan Höving, Thomas Schmidt, Maximilian Peters, Hendrik Lapainis and Norbert Kockmann *

Laboratory of Equipment Design, Department of Biochemical and Chemical Engineering, TU Dortmund University, Emil-Figge-Straße 68, 44227 Dortmund, Germany; stefan.hoeving@tu-dortmund.de (S.H.); thomas6.schmidt@tu-dortmund.de (T.S.); maximilian.peters@tu-dortmund.de (M.P.); hendrik.lapainis@tu-dortmund.de (H.L.)

* Correspondence: norbert.kockmann@tu-dortmund.de; Tel.: +49-(0)-231-755-8077

Abstract: Small-scale continuous apparatuses for solid product manufacturing are receiving increasing interest due to the demand for the fast market availability of specialty chemical products manufactured in integrated and modular processing plants. Relevant unit operations span from crystallization over solid–liquid separation and filter cake washing to drying. For this purpose, the quasi-continuous filter belt crystallizer (QCFBC) was developed and is presented here. The newly integrated unit operations with positive pressure filtration (Δp_{max} = 0.8 bar), filter cake washing ($\dot{V}_{wash}$ = 55 mL·min^{-1}), and convection drying (T_{dry} = 60 °C) have been individually characterized and integrated into the filter apparatus that has been modified for continuous operation. They were synchronized with the flexible cooling crystallization, enabling for a seamless production process. Sucrose in water was used as model substance system. Long-term operations of up to 14 h were successfully performed with dry product filter cakes (22.64 g ± 1.64 g·h^{-1}) of constant quality attributes ($x_{50,3}$ = 216.095 ± 14.766, $span$ = 0.347 ± 0.109, $Y_{rel.}$ = 69.9% ± 5%, X_{RM} = 1.64 mg·g^{-1} ± 1.38 mg·g^{-1}).

Keywords: cooling crystallization; filtration; filter cake washing; filter cake drying; continuous downstream processing; integrated small-scale production

Citation: Höving, S.; Schmidt, T.; Peters, M.; Lapainis, H.; Kockmann, N. Production of Solids, Including Cooling Crystallization, Filtration, Washing and Drying, on a Modular and Integrated Plant. *Processes* **2023**, *11*, 2457. https://doi.org/10.3390/pr11082457

Academic Editors: Ioannis Spanopoulos and Kian Jon Chua

Received: 26 June 2023
Revised: 9 August 2023
Accepted: 10 August 2023
Published: 15 August 2023

1. Introduction

The small-scale production in the fields of fine chemicals and active pharmaceutical ingredients (APIs) have conventionally been conducted in batch operation mode [1–6]. The process understanding generated here covers all relevant unit operations such as solid formation or crystallization, filtration, washing, drying, formulation, etc. Most API manufacturing processes include these [4,7–9]. While continuous processing is state of the art in many disciplines, a significant amount of research effort is still invested in individual continuous small-scale down-streaming for the production of APIs and fine chemicals [8,10,11]. Especially for crystallization concepts, the aim is to also benefit from the advantages that come with continuous processing. These range from an increase in efficiency, consistency in product quality, enhanced product quality control to improved space time yield [5,8,11]. Of course, benefits from batch processes such as high degree of flexibility, lower initial investment cost, and easier product quality control have to be outweighed at the same time [11–13].

The manufacturing of APIs consists in more than a single unit operation in most cases; therefore, the interconnection of several unit operations to one integrated and continuous end-to-end production process is of high interest and potential [14–16]. Next to the benefits that continuous processes already offer, integrated processes additionally offer opportunities such as further increased efficiency, as well as faster innovation transfer and improved supply chain management [6,16–18]. In particular, the transport and storage of

suspensions and slurries containing high portions of solid particles has been a persistent issue in industrial settings, and can be addressed herewith [15,19].

The crystallization in API production routes is the first and most effective way to set crucial properties of the product particles [5,20,21]. Therefore, either preserving these properties or knowing the influences of the following unit operations of solid–liquid separation, washing, and drying on the particles, are a crucial requirement. Thus, not only the thorough investigation of the individual process steps is key to a obtain an intermediate product ready for value-added processing, but also the integrated process as a whole [15,18,22].

The ultimate goal in the pharmaceutical industry and fine chemical production is to create an integrated end-to-end process. This process should have reliable, controllable, and sufficiently characterized downstream unit operations to enable the precise control and conservation of (intermediate) product properties. Besides the selection of contributions that are discussed hereafter, a substantial amount of literature pertaining to the above-mentioned topic can be found in recent, high-quality review papers [6,11,23].

The main concepts recently pursued to achieve small-scale continuous crystallization are either tubular crystallization equipment or (cascaded) vessels with continuous product removal such as draft tube baffle crystallizers (DTBs) and mixed suspension mixed product removal (MSMPR) apparatuses. Tubular setups generally offer narrower residence time distributions (RTDs), while in MSMPR cascades process parameters such as residence time and suspension degree are decoupled and, therefore, offer a higher degree of flexibility [19,20,23].

1.1. Tubular Crystallizers

The coiled flow inverter crystallizer (CFIC) is composed of helically coiled tubing. Multiple individual elements are aligned by bends with a 90° angle serving as a framework for the desired amount of tube coils. This design causes the flow profile to reshape frequently, inducing so-called Dean vortices that enhance the mixing of the process medium. Increasing the number of bends narrows the resulting liquid phase RTD [24]. Hohmann et al. demonstrated that a CFIC (inner diameter: 4 mm, total volume: 80 mL) with flow rates between 1 g·min^{-1} and 10 g·min^{-1} (resulting in residence times (RTs) between 8 min and 80 min) can achieve almost ideal plug flow conditions [24,25]. It was found that the broadening of the product particle size distribution (PSD) highly depends on the flow rate inside the tube. Higher flow rates led to better mixing of the solid phase and more homogeneous RTDs of the solid phase [26].

The slug flow crystallizer (SFC) is also a tubular equipment. Here, the solid carrying liquid is segmented by a second phase, which is gaseous in most cases. The segmented flow induces Taylor vortices inside the liquid slugs that increase the mixing. Additionally, backmixing is limited and narrow RTDs are to be expected in SFC processes [27–29]. Similar effects as described for the CFIC were observed for lower volumetric flow rates that caused L-alanine particles to cluster at the phase boundary causing agglomeration and broadening the product's PSD. Higher slug velocities lead to increased dispersion and the mentioned agglomeration is overcome while uniform crystal growth is promoted [28,29]. In further work, the SFC was integrated with a continuous filter and dryer that will be discussed later [30].

The Archimedes tube crystallizer (ATC) is another tubular concept that does not rely on a common pump for fluid transportation but rather makes use of the Archimedes screw principle [31,32]. An air-segmented suspension medium flow is continuously transported along the apparatus axis while the temperature is consistently decreased to induce cooling crystallization. With a seeded crystallization and flow rates between 11.6 mL·min^{-1} and 55.2 mL·min^{-1}, Sonnenschein et al. were also able to show that increased flow rates lead to better mixing in the suspension and, therefore, less agglomeration of the product particles with more even crystal growth and a narrower PSD [31,32].

Tubular crystallizers with different concepts have been established in the small-scale continuous crystallization processes in research and development. Only few have been successfully commercialized so far [6,33]. An often-cited example is the continuous oscillatory

baffle crystallizer (COBC) by NiTech Solutions Ltd. (Edinburgh, Scotland) [6,34,35]. General concepts from reaction technologies have been adapted for continuous crystallization. Segmented flow plays an increasing role in tubular crystallizers, ensuring increased mixing and narrow RTDs due to minimized backmixing. This partially prevents encrustation, which will always be a challenge in tubular crystallizer equipment [19].

1.2. Cascaded Vessels

The MSMPR crystallizer is often used in a cascaded operation mode where 2–5 vessels are connected according to the plant capacity and cost efficiency [36]. While the RT and other process parameters are mostly decoupled and can be set as desired, the RTD of the product particles is relatively wide [19,36]. Small-scale MSMPRs are part of current research and offer a reliable alternative with more options for process control than the tubular designs; however, they pose challenges regarding technical realization due to miniaturization [12].

Another equipment that is down-scaled to fulfill the requirements of continuous small-scale crystallization [37–39], is the draft tube baffle (DTB) crystallizer which is well known for many industrial applications [1,40]. Usually used for vacuum crystallization, it can also successfully be used in cooling crystallization applications. Longer RT compared to tubular setups lead to lower levels of supersaturation. By using the settling zone and the coupled fine grain dissolution, the product's PSD can be narrowed [21,40].

Generally, due to the different concepts aiming toward continuous processing in cooling crystallization, high potential regarding integrated processes is apparent. The two main concepts, namely tubular equipment or (cascaded) vessels, often seem to either benefit from one of the following: Segmented flow to create separated batches with defined RT or some sort of fine grain dissolution to decrease the amount of small particles in the product and thus narrow the product's PSD. Both concepts have also been incorporated in this contribution.

1.3. Continuous Filter and Dryer

Further along in the downstream process chain, important steps for product formulation are located, where small-scale and continuous equipment is even less discussed in the literature compared to the crystallization step. As these three unit operations are closely interconnected, they are often performed on a single equipment [1] and, therefore, are discussed together in the following step.

The continuous carousel filter dryer (CCFD) is a quasi-continuous filtration, filter cake washing, and drying equipment patented by Alconbury Weston Ltd. [41]. It consists of five cylindrical chambers that can be rotated to five different functional positions, where the process medium is subjected to solid–liquid separation, several washing steps, drying, and finally product discharge [7,33]. As in the common Nutsche filtration, the pressure difference is applied by vacuum from below the filter medium. The operation behavior was characterized by Acevedo et al. and Ottoboni et al. [7,33]. Further studies demonstrated the capabilities for product isolation [42,43], integration of continuous crystallization equipment [44–46], modeling [44,47], and most recently digital design and simulation [47–49]. Due to the quasi-continuous operation, the residence times on each of the positions are coupled and the RT is set by the time spent on each position. Therefore, the product material is clearly traceable as it may be necessary for good manufacturing practice (GMP) applications.

Another small-scale continuous filtration device is the continuous rotary plate filter (CRPF) patented by Continuus Pharmaceuticals [16,50]. Mother liquor and previously added wash medium can be continuously removed at different outlets before the product filter cake is scraped off the rotary plate [16,50]. Due to the limitations implied from further drying the product slurry, it is later resuspended and dried in a continuously coupled rotary drum and vacuum screw dryer [16,50,51]. Recently published contributions show the potential in a heterogeneous crystallization process [50] and the application in end-to-end processes [52].

Finally, the continuous vacuum screw filter (CVSF) is a modular and expandable apparatus for integrated filtration, washing, and drying of product suspensions. It has

been patented by the Chair of Plant and Process Design at TU Dortmund University [53]. It consists of two parts: a rotary polytetrafluoroethylene (PTFE) screw for the axial transportation of the process medium and a tubular glass body. The lower half of the inner jacket consists of a porous filter frit responsible for the separation steps [54]. In a first contribution, Steenweg et al. characterized the filtration capabilities and long-term operability of the equipment [54]. Furthermore, the influence of the filtration on the crystals was found to be minimal. In further contributions, the washing and drying capabilities of the apparatus were demonstrated, yielding free-flowing product particles with a residual moisture between 1 and 2% [54,55]. An actual integration with a previously described tubular crystallizer [27,28] was successful and seems to be a promising concept for an integrated production of crystalline products [30].

1.4. Quasi-Continuous Filter Belt Crystallizer (QCFBC)

To overcome process medium transportation issues and challenges regarding the coupling of crystallization and further downstream processing, we investigate the quasi-continuous filter belt crystallizer (QCFBC) [56,57]. The concept is based on the working principle of a belt filter apparatus and further derived from the Titus–Nutsch–Dryer and the Konfiltro [58,59]. Here, the process medium is segmented by individual containers, equipped with stirrers and sensors, that can be subjected unit operations which have been combined according to a modular approach in equipment design [60]. Previous investigations on the cooling crystallization have demonstrated that the apparatus is capable of reproducible production of product particles [61]. Furthermore, the particle properties were influenced by precise temperature control [57]. For the model substance system sucrose/water, an upscaling study from lab-scale to pilot-scale was performed [62] as well as a population balance model [63].

In this contribution, the quasi continuous and integrated operation of the plant including cooling crystallization, filtration, filter-cake, washing, and drying is demonstrated. Previously determined challenges regarding the washing and drying process have been eliminated by introducing a developed washing, filtration, and convection drying lid of the process containers specifically for this purpose. The successful integration of all of the above-mentioned unit operations in the plant is demonstrated for a quasi-continuous operation with six consecutive containers. Special attention in the analysis is paid to the critical product quality attributes' PSD, relative yield $Y_{\mathrm{rel.}}$, and residual moisture of the filter cake X_{RM}. Furthermore, the long-term operation for 14 h of the integrated plant is presented including all modules for crystallization, filtration, washing, and drying.

2. Materials and Methods

The following chapter will address the design of the plant and the improvements that were made compared to the plant demonstrated in [57], where the focus was on the cooling crystallization. In this contribution, the entire process is considered from solution to dry filter cake. Strategies on characterizing and implementing the downstream steps of filtration, washing, and drying are presented in Figure 1. Next, the quasi-continuous operation principle is introduced.

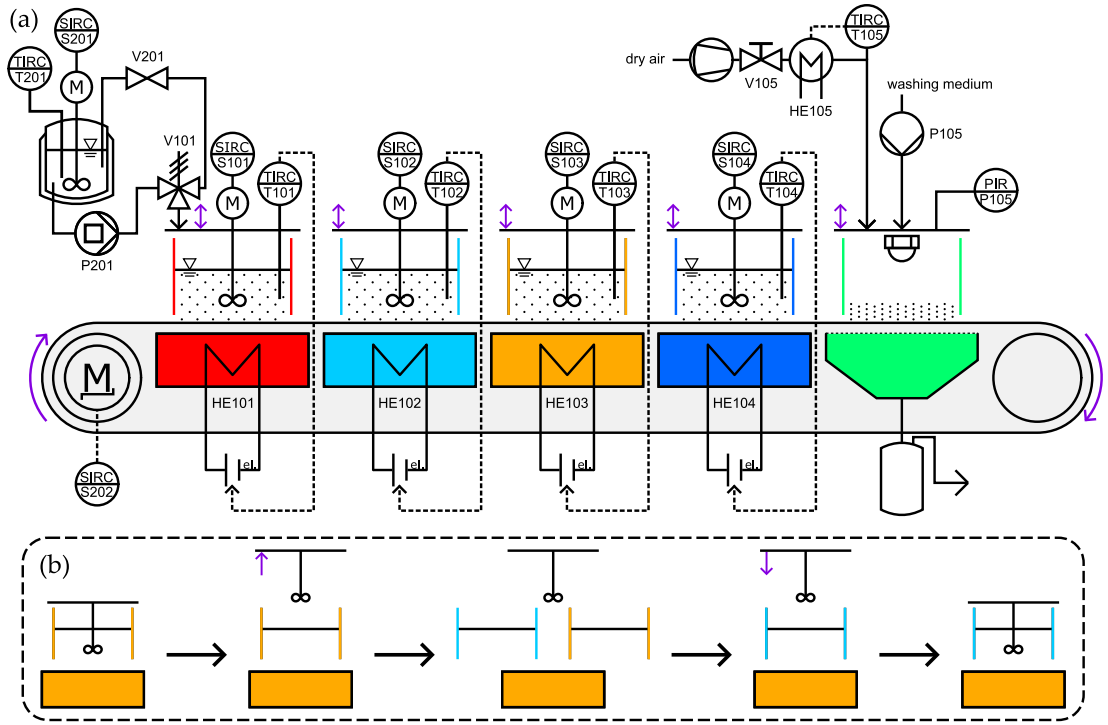

Figure 1. (**a**) Process flow diagram of the quasi-continuous filter belt crystallizer (QCFBC). The functional modular units are displayed in different color. The first four positions are used for cooling crystallization, while the last position (green) marks are where filtration, washing, and drying happen. (**b**) Schematic explanation the container lids´ vertical movement that do not horizontally move with the container. The lid and the bottom cooling/heating module stay at their position and, therefore, need to be lifted while the container moves to the next position.

2.1. Substances Used

The system sucrose/water is chosen as model substance, since it is widely used in various characterization studies. The substances as well as process properties such as solubility, viscosity, crystallization behavior, etc., are well known [57,61,62,64]. To benefit from the already gained experience, the substance system was further used to gain insights and describe the downstream process on the QCFBC. Sucrose was purchased from Südzucker AG, Mannheim, Germany. As solvent, deionized water (<10 $\mu S \cdot cm^{-1}$) was used. To calculate the saturation curve, the following approximation was employed [65].

$$\begin{aligned} c^*[g_{succ} \cdot g_{sol}^{-1}] =& 0.6447 + 8.222 \cdot 10^{-4} \cdot \vartheta + 1.6169 \cdot 10^{-5} \cdot \vartheta^2 \\ & - 1.558 \cdot 10^{-8} \cdot \vartheta^3 - 4.63 \cdot 10^{-10} \cdot \vartheta^4, \ \vartheta \text{ in } ^\circ C \end{aligned} \quad (1)$$

The day before each experiment, the solutions were prepared in a 1 L double jacketed, stirred, and temperature-controlled (ministat 125, Huber Kältemaschinenbau AG, Offenburg, Germany) glass vessel at 10 K above the target temperature. Whenever solid crystals were needed, such as seed crystals or for characterization experiments, they were produced by sieving the sucrose crystals (Test Sieve Retsch, RETSCH GmbH, Haan, Germany). Sieves with pore sizes of 63 µm, 90 µm, 125 µm, and 180 µm were used and the resulting sieve fractions were collected. Whenever the density $\rho(x)$ was needed, the correlation was taken from [66,67].

2.2. General QCFBC Operation Principle

The apparatus used and upgraded in this work has been described thoroughly in a previous work [57]. The general functional principle has already been described in [56,68]. However, since substantial upgrades have been installed and for the sake of comprehensiveness, the apparatus and its working principle will be shortly described.

The functional principle is based on the operation of a horizontal continuous belt filter. The process medium is not continuously introduced to the filter medium but rather separated into batches that are transported along the operation direction of the plant. This way, the individual batches can be treated in additional unit operations rather than only solid–liquid separation. The concept allows for particle formation, filtration, washing, and drying on a single plant in order to connect the process from solutions to a dry filter cake in a well-controlled manner. In order to do so, the filter belt and the attached process container (open to bottom and top) can move between different functional modular units covering the mentioned functionalities. The functional modular units are interchangeable and the process can therefore be custom-tailored to the specific needs of the substance of interest. A process flow scheme is given in Figure 1. From top left vessel, the test solution is pumped by P201 to process medium container 101 that is positioned on the first (red) functional modular unit. Here, the temperature of the suspension is controlled via Peltier elements installed in the modules below the filter belt. After, t_{cycle} all the containers travel to the next position. On the last position (green in Figure 1), the product suspension is filtered and the resulting filter cake is washed and dried. For the last unit operation, a new functional lid was designed that will be described in Section 2.3.

2.3. Experimental QCFBC Setup

The setup is the updated version of the apparatus presented in [57] and parts that are already covered there will only be briefly described here. Installed improvements and amendments will be described more in detail, in particular covering the solid–liquid separation, filter cake washing, and drying on the QCFBC. A rendered CAD drawing of the experimental setup can be found in Figure 2. An image of the complete setup and a video that demonstrates the operation can be found Supporting Material Figure S1, Video S1 (real), and Video S2 (schematically).

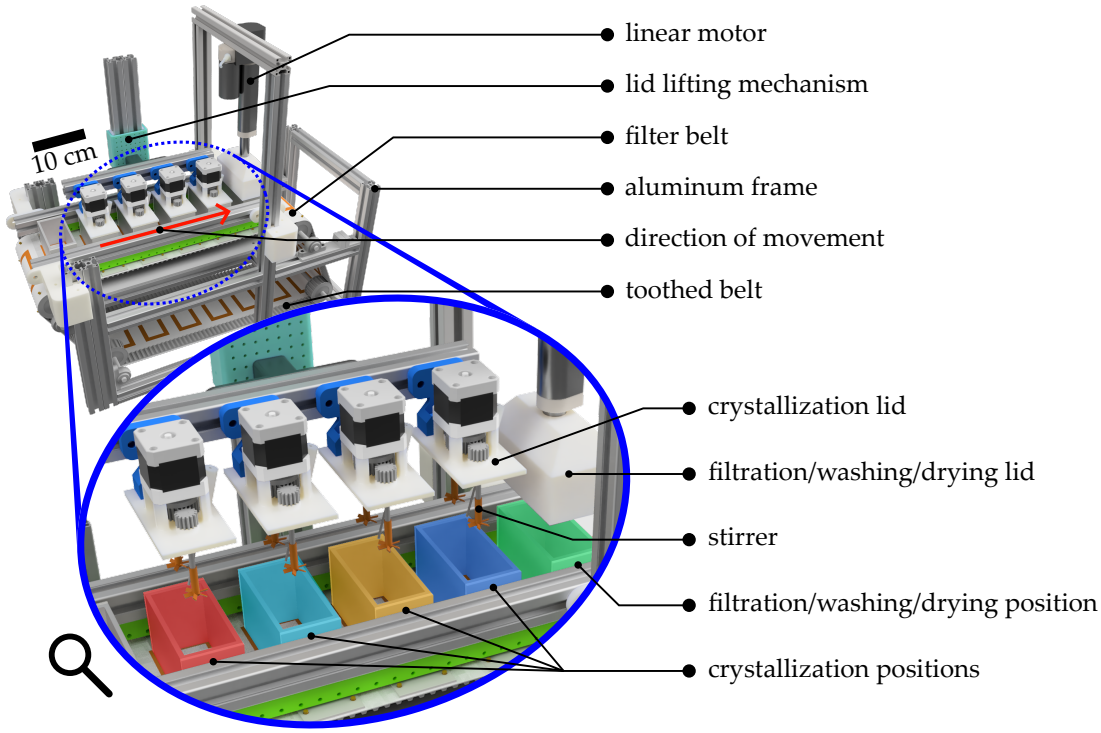

Figure 2. 3D sketch of the modular filter belt apparatus with the four different stirring units, drivers, and aluminum frame. In the detailed view, the container lids are raised. The first four process containers (from left to right in red to blue color) are responsible for the cooling crystallization, while the last container position serves for the filtration, washing, and drying step. The coloring is consistent with Figure 1 .

The main framework of the apparatus is based on common belt filter apparatuses and consists of aluminum profiles (30 mm × 30 mm, Bosch Rexroth AG, Lohr am Main, Germany). Together with the continuous filter belt (SEFAR TETEX® MONO 07-76-SK 022, Sefar AG, Heiden, Switzerland, 22 µm pore size), the process medium container made from aluminum (100 mm × 50 mm × 60 mm (L × W × H), 4 mm wall thickness) can be driven along the apparatus axis. The process medium containers are open at the bottom and top. To prevent the process medium from leaking out of the container, liquid rubber seals (orange liquid rubber, mibenco GmbH, Karlstein am Main, Germany) are applied to the filter belt. In contrast to the setup described in [57], the lids for each of the process container do not travel with the container along the QCFBC. Here, they are automatically lifted before the container changes to the subsequent position where the lids are lowered again. Each lid has two stirrers (pitch blade stirrer, 6 blades, 45°, 19 mm outer diameter, 6 mm shaft, 3D-printed from ABS, coated with mibenco liquid rubber) that were operated at N = 600 rpm resulting in a stirrer Reynolds number between $Re_{stir.,T^*=20\,°C}$ = 27.29 and $Re_{stir.,T^*=60\,°C}$ = 62.01, depending on the viscosity of the solution that was calculated according to the correlation from [69,70].

For precise temperature control, Peliter elements (40 mm × 40 mm × 4 mm, TEC1 127 05, Thermonamic Electronics Corp., Ltd., Nanchang, China) are installed as heat exchangers (Figure 1: HE10X) in the crystallization modules. Pt100 (Pt-B-100-2, Rössel Messtechnik GmbH, Dresden, Germany) temperature sensors were installed in the lid and reach into the suspension while it is in the lowered position. For process control and automation, the lab automation system, LabManager®, and the software LabVision® are used (HiTec Zang GmbH, Herzogenrath, Germany). More detailed information on the experimental setup can be found in the previous work [57].

Filtration, Washing, and Drying

The second major improvement next to the mechanism responsible for the movement of the container lids was the upgrade on the last module position on the apparatus. As experiments have shown, contact drying of the filter cake as it was intended or performed in [56,57,62] was inefficient and resulted in filter cakes with high residual moisture. Therefore, the contact drying modules were omitted and a convection drying system was installed, which can be used on the filtration module. An explosion drawing of the setup can be seen in Figure 3 with the view from below.

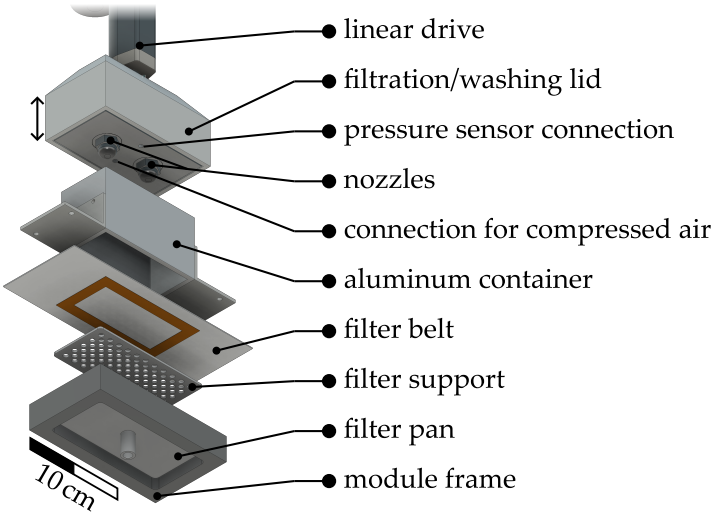

Figure 3. Exploded view of process medium container on the filtration, washing, and drying module. The lid can be pressed on top of the container and seals the process compartment airtight, enabling for the application of a pressure difference and washing medium through the nozzles.

The linear drive (DSZY1-24-40-100-STD-IP65, MSW Motion Control GmbH, Werther (Westf.), Germany) presses the lid on top of the container with up to 1000 N, ensuring a sealed atmosphere inside the process compartment. To support this, the lid is covered with a silicone sealing (3 mm thick) from below. For filtration and drying, dry air from the central pressurized air network is used. With valve V105 (MS4-LR, Festo SE& Co. KG, Esslingen, Germany), a desired pressure difference during the filtration ($\Delta p_{\text{filt.}}$), washing ($\Delta p_{\text{wash.}}$), or drying (Δp_{dry}) between the sealed space and the outside can be set and tracked with P105 (A-10, WIKA Alexander Wiegand SE& Co. KG, Klingenberg am Main, Germany). Pressure differences of up to 800 mbar have been used for filtration. Since pressurized air was already used for the filtration, it was employed for convection drying, too. To increase the temperature of the drying air up to 80 °C, HE105 was 3D-printed (High Temp V2, Formlabs GmbH, Berlin, Germany) and equipped with an electric heating element (PTC-Heating Element, Tru Components, Hirschau, Germany). An illustration of this can be found in Supporting Material Figure S2.

For filter cake washing, two hollow cone spray nozzles (220.085.11.AC, Lechler GmbH, Metzingen, Germany) were installed in the lid at the same transversal positions as the stirrers in the crystallization lids. Washing liquid is pumped by a double position pump (SyrDos, HiTec Zang GmbH, Herzogenrath, Germany). Different volume flow rates in the range from 55 mL·min^{-1} to 100 mL·min^{-1} were used in filter cake washing experiments. According to the manufacturer, a full cone spray is to be expected at these relatively low flow rates.

2.4. Experimental Procedures

Regarding the experiments, this contribution can be divided into two parts. The first part describes characterization experiments performed to identify capabilities and optimal operation parameters. This mainly covers filtration, washing, and drying since cooling crystallization has been covered in [57]. The second part addresses the quasi-continuous operation of the plant plant that aims toward a complete production process chain from mother liquor to dry filter cake.

2.4.1. Characterization: General

Since filtration, washing, and drying have not yet been investigated thoroughly on the plant of interest, they will be described in this contribution. In order to exclude possible influences due to the cooling crystallization beforehand, product suspensions have been "artificially" produced by suspending sieved crystals in saturated sucrose solution. Sucrose particles from the sieve size fraction of 125–180 µm have been collected which are in the same range as product crystals from [57]. To simulate a completed crystallization $m_{\text{FC,max}}$ = 24.27 g ± 0.09 g of these were used as solid product particles, where

$$m_{\text{FC,max}} = ECM_{\text{max}} + m_{\text{SC}}. \quad (2)$$

The parameter m_{SC} is the seed crystal mass, while ECM_{max} is the maximum excess crystal mass for the relevant experimental setting, calculated as

$$ECM_{\text{max}} = (X^*_{\text{start}} - X^*_{\text{end}}) \cdot m_{\text{ML}} \cdot x_{\text{aq}}, \quad (3)$$

with X as loading, m_{ML} as mass of the mother liquor, and x_{aq} as the water content of the liquid phase. For T_{end} = 20 °C it was calculated that $m_{\text{ML,20 °C}}$ = 77.31 g, which was used as mass for the saturated liquid phase and is equivalent to the ideal product suspension properties. These conditions were used for the primary characterization experiments, where different process parameters for filtration, washing, and drying were screened. Before the experiments, the solution was filled into the process container on the last temperature module on the plant and the suspension temperature was set to T_{end} = 20 °C. After the temperature was reached, the previously prepared solid sucrose was added and thoroughly suspended for 4 min with the installed stirrers. Then, the container with the suspension

was moved forward to the subsequent module, where the following unit operations were performed and investigated.

2.4.2. Characterization: Filtration

For the solid–liquid separation, the positive pressure filtration was imposed by the lid and the pressurized air network was benchmarked against the negative pressure filtration as it was used in [57]. Here, a vacuum pump (PC3001 VARIO^{pro}, VACUUBRAND GmbH & Co KG, Wertheim, Germany) was used to create the necessary pressure difference. The behavior of the filtration regarding moisture reduction in the filter cake was investigated for different filtration times ranging up to 20 min. Additionally, three different pressure difference levels (0.4 bar, 0.6 bar, 0.8 bar) were studied. Therefore, the measured pressure of the vacuum pump and the pressure sensor P105 were recorded. The mass of each filter cake was determined at different points during the process. The residual moisture X_{RM} was gravimetrically determined according to

$$X_{RM} = \frac{m_{FC} - m_{FC,dry}}{m_{FC,dry}}, \quad (4)$$

with the mass of the filter cake of interest m_{FC} and the mass of the dried (at least 2 weeks at 600 mbar and 60 °C) filter cake $m_{FC,dry}$. To reproducibly measure the weight of the filter cake throughout the filtration experiments, a frame for the filter belt was 3D-printed. With this setup, the container and cake could be removed from the apparatus and safely moved to the scale (Kern 572, KERN & SOHN GmbH, Balingen-Frommern, Germany). An image of the installed frame can be found in Supporting Material Figure S3.

2.4.3. Characterization: Washing

The distribution of the washing medium on the filter cake was investigated regarding the washing performance of the setup. The applied washing liquid was collected in a custom well plate, positioned where the filter cake would be in an actual washing procedure. An image of the partly 3D-printed assembly can be found in Supporting Material Figure S4.

During the experiments, it became clear that mother liquor remained in the filter cake of the succhrose/water system to a high degree. Therefore, the wash out experiments focus on removing the mother liquor from the filter cake, treating the dissolved sucrose as "contamination". Wash out experiments were performed with ethanol (99%, VWR International GmbH, Darmstadt, Deutschland) and deionized water (<10 µS·cm^{-1}) as washing medium. In case of water as washing medium, methylene blue (99.9%, Thermo Fischer Scientific, Waltham, MA, USA) was added to the filter cake, forming a sucrose suspension at a concentration of 0.03 mg·mL$_{sol.}^{-1}$ as a tracer. The tracer concentration of the collected wash medium was optically measured (Cary 60 UV-Vis Spectrophotometer, Agilent, Santa Clara, CA, USA). Assuming the concentration of the sucrose in the mother liquor $c_{suc.,wash,i}$ to be proportional to the concentration of the tracer $c_{tracer,i}$,

$$c_{suc.,wash,i} \propto c_{tracer,i}, \quad (5)$$

it is possible to distinguish between the sucrose that stems from the mother liquor remaining in the filter cake and the sucrose that dissolves from the filter cake during the washing. Wash ratios,

$$W = \frac{V_{wash}}{V_{pores}}, \quad (6)$$

of up to 3 have been investigated. Here, V_{wash} is the volume of used wash medium and V_{pores} is the pore volume of the filter cake. For the characterization of the different washing parameters, the ratio of the remaining contamination m_X divided by the pure filter cake mass m_{solid} as

$$X = \frac{m_X}{m_{solid}}. \quad (7)$$

To standardize this, X is set into relation with the loading of a fully saturated filter cake (X_0):

$$X_i^* = \frac{X}{X_0} = X_{i\text{-}1}^* - \frac{m_{suc.,wash,i}}{m_{suc.,ML,0}}, \text{ for } i \geq 1 \quad (8)$$

where $m_{suc.,ML,0}$ is the mass of sucrose that remains in the pores of the filter cake as mother liquor and calculated as

$$m_{suc.,ML,0} = V_{FC} \cdot \left(1 - \frac{m_{suc.,FC}}{V_{FC} \cdot \rho_{suc.}}\right) \cdot \rho_L(x) \cdot x_{suc.,ML,0} \quad (9)$$

The mass of the sucrose washed from the pores of the filter $m_{suc.,wash,i}$ cake can be calculated according to

$$m_{suc.,wash,i} = \frac{c_{suc.,wash,i}}{\rho_L(x)} \cdot m_{water,i} \cdot \left(1 - \frac{c_{suc.,ML,washed,i}}{\rho_L(x)}\right)^{-1} \quad (10)$$

X_0 is calculated as the ratio of contaminant ($m_{suc.,0}$) divided by the mass of particles (m_p) in the filter cake.

To avoid wash liquid buildup above the filter cake, the positive pressure difference from the previous filtration was unchanged (0.05 bar–0.02 bar) during the characterization experiments. For the washing step itself, the wash liquid flow rate was set to 55 mL·min^{-1} after 1 min of solid–liquid separation. Due to the preceding filtration, the pores of the filter cake were not saturated with liquid at the beginning of the washing step.

2.4.4. Characterization: Drying

As mentioned before, the convection drying was also implemented on the filtration, washing, and drying module. To benchmark the performance of the newly integrated drying, it was compared to the performance of the contact drying that was implemented by Dobler et al. [56]. Both options were therefore incorporated into the plant for this contribution. Due to the modular concept, both mehtods can be simply interchanged. To have the same starting conditions for the filter cakes that undergo the drying experiments, the previously stated settings hold here, too. The preceding filtration was also performed with constant temperature and pressure conditions for 5 min, with the vacuum pump at 0.4 bar abs. The contact drying at 60 °C served as benchmark, while the convection drying was investigated at room temperature (≈20 °C) and 60 °C. To increase the temperature of the air used for convection drying, a heat exchanger HE105 was custom-built and equipped with a PID-controller. More details on this can be found in Supporting Material Figure S2. For the calculations of the residual moisture, the same equations as for the filtration hold. Only here, the change in residual moisture as

$$\Delta X_{RM} = X_{RM} - X_{RM,0}, \quad (11)$$

was calculated to make the results more comparable. The masses were determined gravimetrically as described before. While investigating the contact drying module, it was disassembled from the plant and placed on top of a scale (Kern 572, KERN & SOHN GmbH, Balingen-Frommern, Germany) to receive continuous data on the residual moisture (a supporting image can be found in Supporting Material Figure S3). As for the convection drying, the removable filter frame was used, and the mass was incrementally determined every 20 min.

2.4.5. Quasi-Continuous Experiments

After the cooling crystallization has been characterized in [57] and further downstream steps have been characterized in this contribution, the complete quasi-continuous operation on the QCFBC was still pending to perform the entire production process. The modular and integrated design of the plant is the base for this approach. For the quasi-continuous

experiments, n_{batch} = 6 container were introduced to the QCFBC one after the other in series every t_{cycle}, so that each experiment with $n_{mod.}$ modules on the QCFBC takes $t_{tot.}$:

$$t_{tot.} = n_{mod.} \cdot t_{cycle} + (n_{batch} - 1) \cdot t_{cycle} \quad (12)$$

This time, summation results in 300 min for t_{cycle} = 30 min, which was the standard setting for the conducted experiments. As a more product-oriented alternative to constant module temperatures as presented in [56,61,62], the temperature profiles were modified related to [57], where the suspension temperature was controlled. The temperature profiles can be seen in Figure 4. The oscillating profile now has a point symmetry at $t = 60$ min. This was performed in a way that the temperature profiles for each individual batch can be proceeded on the next module without major disturbances by passing on the container at 40 °C. Later, it was discovered that, against all expectations, small jumps in the temperature profile as seen in Figure 4b,c do not cause major issues for controlling the temperature.

The preheated (70 °C, saturated at 60 °C) sucrose solution was manually filled into the module container with a preheated single-use 100 mL syringe (B.Braun SE, Melsungen, Germany), where the solution temperature was controlled according to the respecting temperature profile starting at 59 °C. The use of P201, V101, and V201 of the feed line, was omitted in the experiments to have precise knowledge about the introduced suspension mass, which is important for mass balance calculations. After the first 10 min of temperature control, the seed crystals were added to the solution through a dedicated hole in the stirrer lids. The next manual step in the process chain is taking the dried filter cake and the container from the filter belt after the drying module. A summary of the relevant process parameters can be found in Table 1.

Table 1. Operating parameters for the quasi-continuous and long-term experiments in this contribution that were used if not stated otherwise.

Unit Operation	Operating Parameter	Value	Description
Cooling Crystallization	T_{start}	59 °C	start temperature
	T_{end}	20 °C	end temperature
	$n_{stirr.}$	600 rpm	stirrer speed
	V_{batch}	74.33 mL	sucrose solution volume
	m_{sc}	0.567 g	seed crystal mass
	x_{seed}	90–125 µm	seed crystal sieve fraction
	$t_{cryst.}$	120 min	crystallization process time
	$T(t)$	oscillating	temperature profile
Solid–Liquid Separation	$t_{filt.}$	5 min	filtration time
	$\Delta p_{filt.}$	0.8 bar	filtration pressure difference
Washing	t_{wash}	20 s	washing time
	$\dot{V}_{wash}$	55 mL·min^{-1}	washing medium flow rate
Drying	T_{dry}	60 °C	temperature of drying air
	t_{dry}	24.67 min	drying time
	Δp_{dry}	$\geq$ 0.4 bar (resulting)	pressure difference during drying
Overall Process Parameters	t_{cycle}	30 min	time spent on each module
	$n_{mod.}$	5	amount of modules installed
	$n_{mod.,cryst.}$	4	amount of crystallization modules
	n_{batch}	6	total amount of container used
	$t_{tot.}$	150 min	total time on the QCFBC

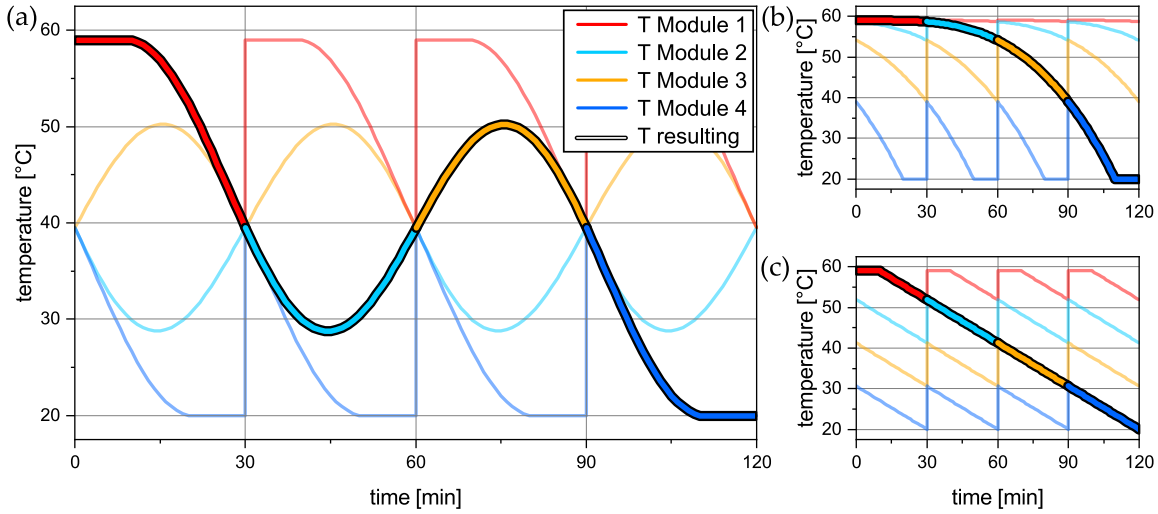

Figure 4. Target temperature of the crystal suspension on the four continuously operated temperature modules. Each color represents one temperature module. The framed (bold) profile is the resulting temperature profile each container experiences when moving across the four modules. (**a**) Oscillating profile, (**b**) progressive profile, (**c**) linear profile.

2.5. Process Analytics

To determine the particle size distribution (PSD) during the crystallization process, samples of 0.5 mL were drawn from the containers every t_{cycle} with a single-use pipette (VWR International, Radnor, PA, USA). According to the protocol described in [57], the solids were separated from the mother liquor and prepared for PSD determination via sedimentation analysis with a LUMiReader® PSA453 (LUM GmbH, Berlin, Germany). The liquid filtrate was used for the determination of the yield according to

$$Y_{\text{filtrate,rel.}} = \frac{m_{\text{ML}} \cdot x_{\text{aq.}} \cdot (X_{\text{start}} - X_{\text{end}})}{ECM} \cdot 100\%, \tag{13}$$

so that information on CSD and the yield is available during the crystallization process. For the quasi-continuous experiments, this was performed for only the third of the six containers due to high manual workload. During the long-term experiments, samples were taken for each container from the product suspension right before the filtration, omitting the samples during the process, gaining information on each product batch. The water mass ($m_{\text{ML}} \cdot x_{\text{aq.}}$) was gravimetrically determined as described before.

The yield can also be determined from the obtained filter cake at the end of the process in an analogous manner:

$$Y_{\text{FC,rel.}} = \frac{m_{\text{FC}} - m_{\text{SC}} - m_{\text{FC,ML}}}{ECM} \cdot 100\% \tag{14}$$

This was performed for each experiment.

3. Results and Discussion

The presentation of the experimental results and their interpretation is divided into three subsections. In the first section, the individual unit operations that have not been covered so far are characterized . Second, the results of the quasi-continuous operation of the entire plant with focus on the critical product quality attributes and plant operability are presented. Finally, the long-term operation of the plant will be presented and discussed.

3.1. Characterization of Unit Operations

Since the cooling crystallization has been covered in [57], details will be left out at this point, but can be found in Section 3.2. In the following, the results of the characterization experiments of the subsequent unit operations will be described. To mitigate the influence of the crystallization step, the processed suspension was created with sieved crystals representing the product properties of the actual crystallization process.

3.1.1. Filtration

The solid–liquid separation was performed via a vacuum applied from the filtration module originally as presented in [57,71]. Here, the filtration with positive pressure applied from above the suspension and filter cake was additionally considered. This method offers benefits regarding the subsequent washing and drying step. The pressure curves for both setups and different pressure differences can be seen in Figure 5a. It can be observed that the set pressure can be reached faster by the positive pressure setup, since it is more rapidly available due to the pressurized air network. For the vacuum pump, the filter cake is even deliquored before the target pressure of 0.2 bar is reached. After that, the pressure climbs back to ca 0.9 bar. The constant pressure difference of ca. 0.1 bar from ambient pressure for all experiments after 2 min confirms the assumption of similar filter cake properties. Standard deviations, plotted as shades, are within a comparable range. As expected, higher pressure differences lead to a faster deliquoring of the filter cake.

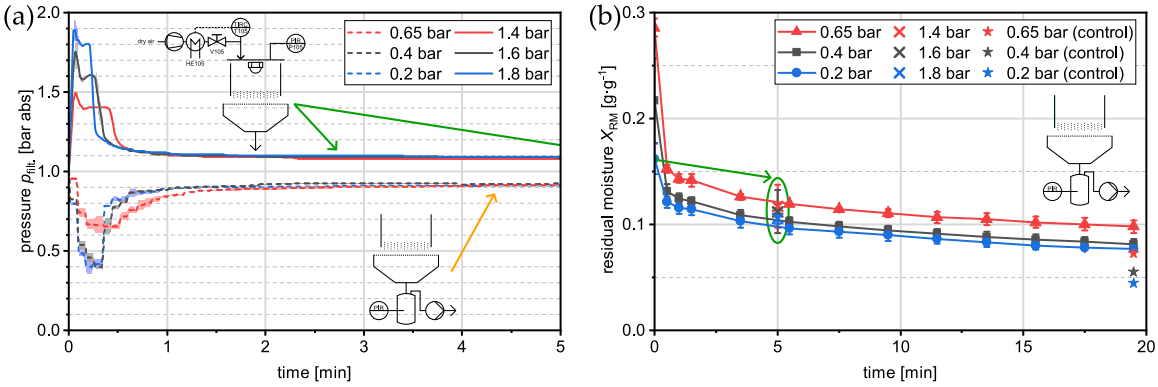

Figure 5. Pressure curves of positive and negative pressure filtration are shown in (**a**) for different pressure levels. The standard deviation from four experiments is indicated as the shadow around the curves. In (**b**), the water content in the filter cakes is plotted versus the filtration time. The measurements were started right after applying the pressure difference to the filter. The standard deviation from four experiments are indicated by the whiskers. The control experiments represented by the stars have been performed one-fold without sampling during filtration.

In Figure 5b, the water content in the filter cake is displayed over the filtration time. One can clearly see that higher pressure differences in the filtration lead to lower residual moistures. Since for the vacuum filtration the filter cake was taken from the setup to be weighed for sampling, the experiments have been repeated without sampling. These results are marked as stars in Figure 5b. One can see that the sampling has an influence on the outcome of the results in a negative manner regarding the residual moisture. However, the magnitude of less decreased residual moisture is consistent for all settings. This also holds for the positive pressure filtration that yielded results within the same range as the vacuum filtration after 5 min. The results are consistent with Darcy's law stating that the pressure drop in the filter cake only depends on the pressure difference $\Delta p_{\text{filt.}}$.

Overall, no substantial difference between both setups, looking only at filtration, was found. The results from the original filtration module [57], using the vacuum pump, are reproducible with positive pressure filtration. The positive pressure filtration setup was used for further investigations due to additional benefits:

- Reproducible air properties;
- Air temperature controllable;
- Pressure differences >1 bar possible;
- Less experimental effort;
- Integration with washing and drying possible.

In comparison with negative pressure from vacuum with high effort, the above-mentioned points led to a robust filtration process.

3.1.2. Washing

Due to the high viscosity (207.8 mPa·s) of the sucrose mother liquor at 20 °C [72], non-negligible quantities of it stay in the pores of the filter cake after the filtration. To benefit from the properties of the primary particles obtained from the cooling crystallization, the filter cake washing step was integrated to displace the mother liquor from the filter cake. The goal is to reduce aggregation and agglomeration inside the filter cake to a minimum without negatively influencing the filter cake itself, by tracking the amount of displaced mother liquor from the pores.

Firstly, the distribution of the sprayed washing liquid was investigated since the application of in a rectangular container is not trivial. A setup with two spatially equally distributed spray hollow cone spray nozzles (Lechler GmbH) was used. The sprayed water was collected at the vertical position of the filter cake. The application area was divided into rectangles by a 3D-printed well plate (Supporting Material Figure S4) and the water was collected. The results of the collected water amount relative to the total amount are given in Figure 6. One can clearly see the effect of the spray cones of the two nozzles that distribute the sprayed water in a circular cone around the projected nozzle position (indicated by a red dot), although the flow rate is at the lower limit of the operation window advised by the manufacturer of the spray nozzle. In particular, the corners of the rectangular area receive less washing water.

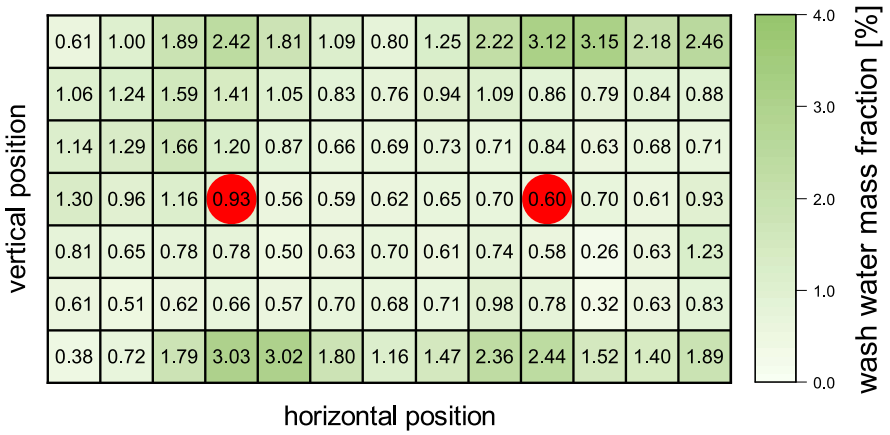

Figure 6. Distribution of the washing liquid on the filter cake surface. The sprayed water was collected with a 3D-printed setup that can be found in Supporting Material Figure S4. The positions of the nozzles are indicated in red. The results shown are averages from triple experiments, in which 91 incremental volumes have been investigated. As the legend suggests, a darker shade of green represents a bigger volume fraction of water in the individual position.

Secondly, the influence of the washing on the "impurities"; here, the sucrose in the mother liquor remaining in the pores of the filter cake, was investigated. The results of these examinations can be found in Figure 7. The product of interest and the impurity are the same substance, which is challenging in the experiments, since solvents dilute the mother liquor but dissolve the filter cake at the same time. Not only water as a washing liquid was investigated but also ethanol in which sucrose has a low solubility [73]. The washing curves can be seen in Figure 7 in gray dashed (ethanol) and solid (water) lines. These curves are

far from the ideal curves as they are given in dedicated contributions [74,75]. However, with both washing liquids, it is possible to reduce the content of sucrose in the pores. For ethanol, the concentration loading X^* stays constant for the last two measurements with a low standard deviation, indicating that the limit by displacement washing is reached for this system. Subsequent effects in washing, such as diffusion washing, do not play any role due to the low solubility of sucrose in ethanol. With water as the washing medium, the loading X^* continues to decrease for all measurements. Here, effects such as the dilution washing play an important role. However, the washing water also dissolves the filter cake. Regarding the wash ratio W, the change in pore volume of the dissolving filter cake is not taken into account at this point.

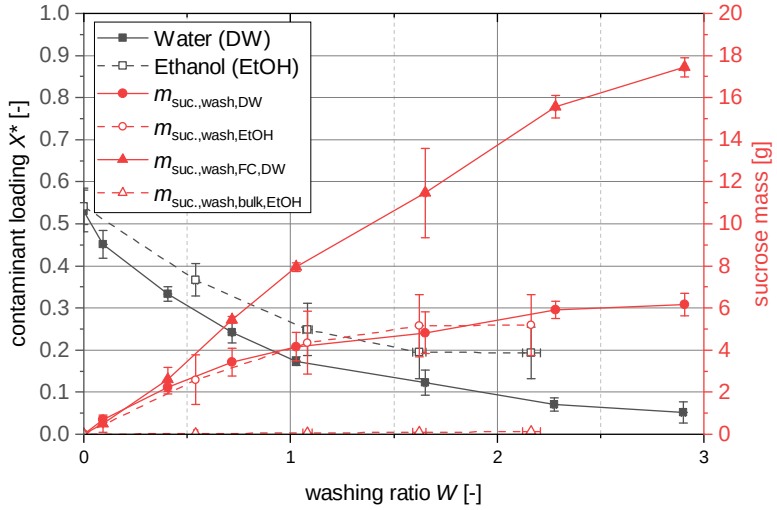

Figure 7. Washing curves (gray) of the unsaturated filter cakes. The dissolved sucrose solution is treated as the "impurity". Pore volumes (and therefore W) for the shrinking filter cake are not adjusted. In red, the collected sucrose mass is plotted. Solid symbols represent the mass washed from the filter cake pores while the outlined symbols stand for the mass that is washed from the filter cakes.

By using the tracer in the mother liquor and the assumptions stated in Section 2.4.3, it was possible to distinguish between the sucrose coming from the mother liquor and the sucrose dissolved from the filter cake. These masses are plotted in solid lines in Figure 7. One can clearly see that the washed mass from the mother liquor is the same for ethanol and water until it stagnates for ethanol due to the lack of diffusion. For reference, a previously not suspended "filter cake" labeled as bulk has been washed with ethanol as a worst case scenario regarding the dissolution of the filter cake itself. The washing liquid was collected and the sucrose content washed from the bulk can be found in the diagram ($m_{suc.,wash,bulk,EtOH}$). It is also clearly visible that water as a washing medium also highly reduces the mass of the filter cake (23.26 g) to where there is almost no filter cake left. For any further experiments, the filter cake was washed with ethanol, which allowed for successful washing without dissolving the filter cake to a high extent.

3.1.3. Drying

In previous contributions, the wet filter cake was further deliquored by a drying step on a dedicated drying module [56,57,62]. The filter cake was moved to a heating module that applied heat to the filter cake, aiming to reduce the residual moisture. The newly implemented filtration and washing module is also capable of convection drying with conditioned air, which was benchmarked against the contact drying from the previous setup. The drying results can be found in Figure 8. The investigated filter cakes have been produced by the same procedure as before with a vacuum filtration of 5 min. The change in

water content was determined gravimetrically with regard to the initial weight and it is plotted on the ordinate.

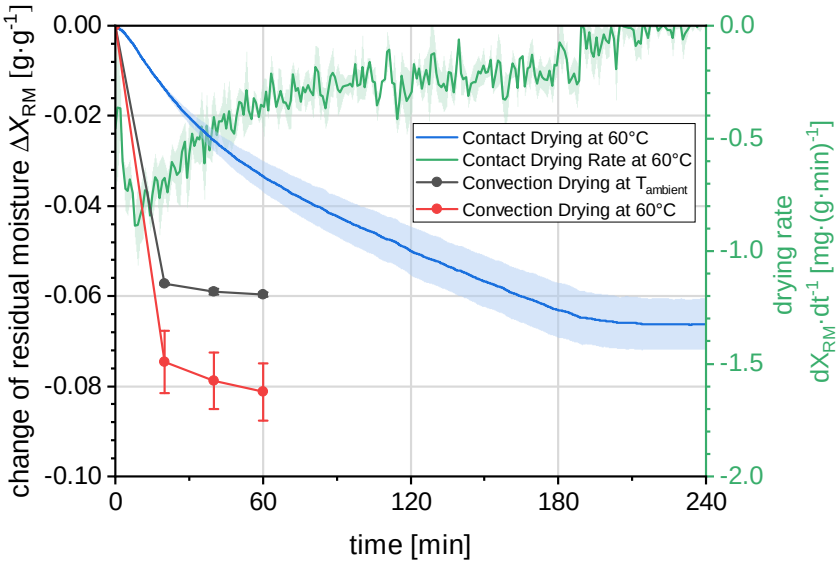

Figure 8. Change in residual moisture of equally produced filter cakes for contact drying and convection drying at different temperatures. The indicated standard deviations stem from triple experiments. For the convection drying, the pressure above the filter cake was set to Δp_{dry} = 200 mbar.

For the contact drying with a module temperature of 60 °C, the residual moisture constantly decreases with a decreasing rate after 10 min (Figure 8 green line). The time before that, the filter cake was heated up. After ca. 200 min, a steady state for the residual moisture is reached where it does not further decrease. Regarding the contact drying, the timescale of ca. 3 h for steady state exceeds t_{cycle} by far and would thus entail the installation of further drying modules for the quasi-continuous operation trying to reach the steady state. For the convection drying with air from the pressurized air network, the reduction in the water content in the filter cake was increased by more than 300% after 20 min in comparison to the contact drying. When increasing the air temperature to 60 °C, the water content was reduced more in 20 min than the contact drying reached after 240 h. Comparing convection drying at 60 °C to the contact drying at 20 min, an increase of 430% was reached. A duration of 20 min is well in the range of possible t_{cycle} and increased reduction in moisture in the filter cake was achieved. Therefore, the convection drying was selected for further experiments.

3.2. Quasi-Continuous Operation

Based on the results from the characterization experiments for each of the unit operations, the operation parameters have been selected for the quasi-continuous operation. In these experiments, slight modifications of the temperature profiles in [57] have been used to fit the constraints of the continuous operation. In this chapter, one experiment represents a single run that has been operated with six consecutive containers, which have gone through all previously characterized unit operations. Relative yields $Y_{rel.}$ as well as residual moistures X_{RM} have been determined for each batch, while the PSD and the sucrose concentration and, therefore, $Y_{filtrate,rel.}$, have been determined gravimetrically for the third container at each t_{cycle}, respectively. Especially for solid–liquid separation, washing, and drying, in-depth investigations were feasible only to a limited extend. For investigations in the same range as in the characterization experiments of the individual unit operations, too many interventions in the process would have been necessary, disturbing the overall process. Therefore, the focus here is on the quasi-continuous operation in terms of feasibility and consistency. The operation parameters can be found in Table 1.

3.2.1. Cooling Crystallization

The cooling crystallization concept on a single module with a sophisticated parameter study has been presented in [57] and a mechanism to continue the temperature profiles on subsequent modules has been proposed. Here, the full temperature profiles were operated on four modules with six consecutive containers instead of one. In the bottom panels of Figure 9, the results for all three temperature profiles are demonstrated as an average from 18 experiments (Figure 9a–c). The position switch of the containers from module n to module $n+1$ is indicated by the vertical line in the diagram. The position change takes approx. 20 s, wherein the temperature sensors are not submerged anymore. The oscillating temperature profile was modified so that the temperature at the "transfer times" is 40 °C. Hence, there is no temperature difference in the suspension that needs to be covered by the subsequent module. However, it is clear that all three respective temperature profiles can be continued on the subsequent module without major interruptions. The only deviation from the target temperature profiles can be found in the beginning of the profiles, where the target temperature of the freshly filled mother liquor is 59 °C. Here, the controller has a slight undershoot within the first 5 min of the profile. Since the seed crystals are introduced at 10 min, where the target temperature is met again, this temporary temperature decrease has no influence on the crystallization. Spontaneous nucleation has not been observed. It can be concluded that the implementation of the control strategy led to a well-executed temperature profile, although it was executed on four different modules, which lays the foundation for the quasi-continuous operation of the plant.

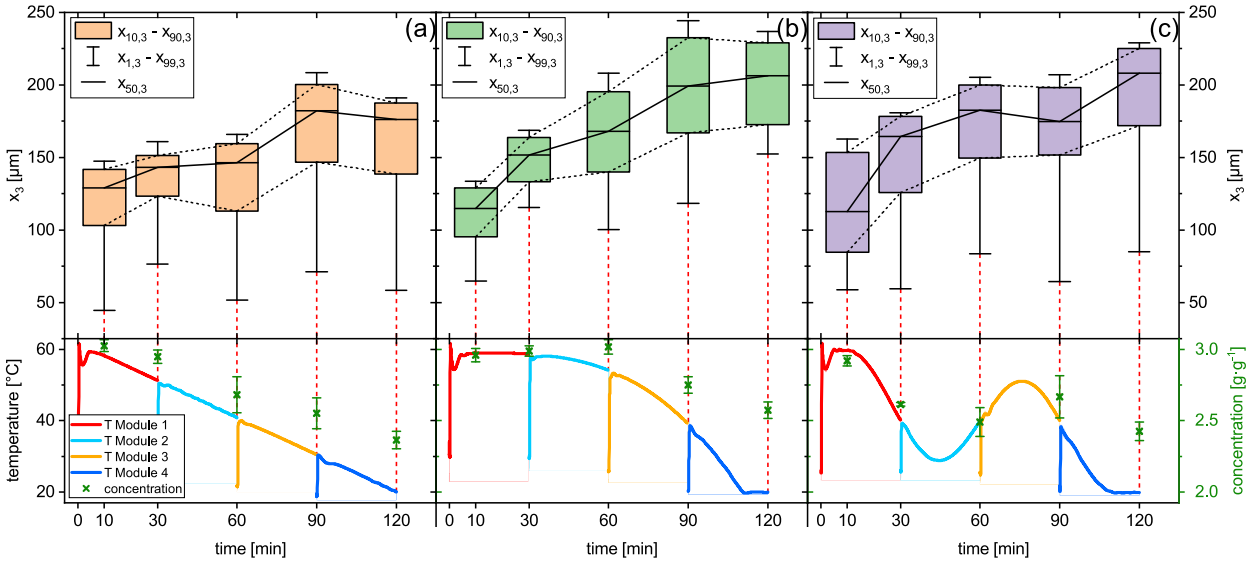

Figure 9. PSDs as boxplots for the linear (**a**), progressive (**b**), and oscillating (**c**) temperature profile in the respective top panels. The bottom panels show the average temperature profile (standard deviations plotted but not visible) for each of the 4 modules (coloration is consistent with Section 2). The temperature profile has a vertical line, where the container was moved to the next position, and the temperature sensors were withdrawn from the suspension. Additionally, the concentration of the liquid part of the suspension is plotted analogous to Equation (13). $t_{cycle} = 30$ min, $n_{stirr.} = 600$ rpm, $m_{sc} = 0.567$ g, $x_{seed} = 90$–125 µm.

The concentration of the solution was gravimetrically measured from the third container of each experiment, which is also plotted in the bottom panel in green crosses. In general for all profiles, the concentration decreases in the solution indicate the growth of sucrose crystals. The concentration after the crystallization is the highest for the progressive profile, while the other two profiles end up at about the same level at ca 2.4 $g \cdot g^{-1}$. The temperature decrease in the second half of the progressive profile seems to be too high for the crystallization kinetics to reduce the supersaturation accordingly. The concentration

profile of the oscillating profile shows that the concentration increases in the solution after it was reheated, as intended. To have an in-depth look into this, a more detailed investigation on the concentration of the solution during the oscillating profile was made. The interpreted results are plotted in a T-c-diagram with the saturation curve and can be found in Section S5 of the Supporting Materials.

In the top panels of Figure 9, the evaluated PSDs, each evaluated according to the sedimentation method of every third tank, are shown as boxplots. Here, the growth of the particles can be seen for all three temperature profiles. Although the supersaturation at the end of the process is the highest for the progressive profile, the fraction of fines is the smallest. The low slope of the profile in the first half of the profile caused the growth of existing crystals instead of the formation of new crystals, as it can be seen in the other profiles. Later on, the growth and particle formation kinetics were too slow to decrease the supersaturation, resulting in large and narrow distributed product crystals with a low relative yield (comp. Figure 10).

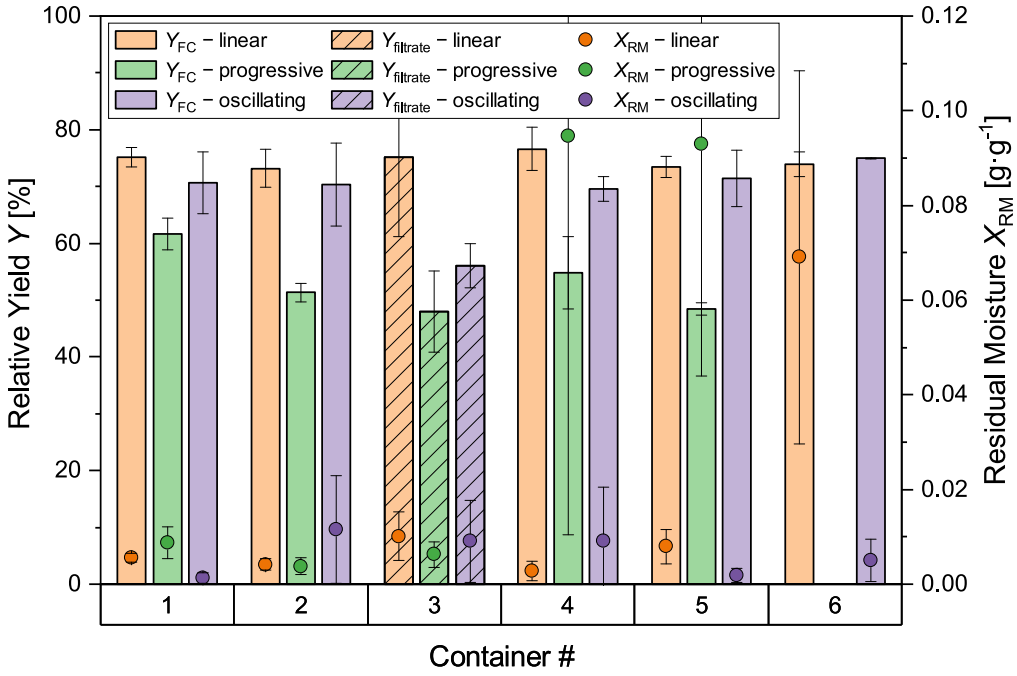

Figure 10. Yields Y and residual moisture X_{RM} of the filter cakes for the six containers for each of the experiments (triplets) determined gravimetrically. For each third container, $Y_{filtrate}$ was determined via the filtrate (hatched bars) of the solution instead of the filter cake (Y_{FC}) (non-hatched bars).

The oscillating temperature profile aims toward resolving the fine fraction with the reheating cycle, narrowing the PSD as it was demonstrated in [57]. Although a decrease in size for the larger particles is observable, the fine fraction does not decrease. However, the lowest concentration and, therefore, the highest relative yield as well as the largest product particles were achieved across the three investigated profiles. Hence, for the long-term operation, the oscillating temperature profile was selected.

3.2.2. Filtration, Washing, and Drying

The further down-streaming unit operations after the crystallization have been performed on the same module and, therefore, the relative yield (Y_{FC}) and the residual moisture (X_{RM}) after the drying of the filter cake were investigated gravimetrically. The respecting results, broken down according to the container number, can be found in Figure 10. Here, one can observe the trends that were also visible with the measured solution concentration in Figure 9. The yield Y_{FC} for the linear and oscillating profile range is in the same region of 70–80%, while the yield for the progressive profile is lower than 50%, as explained

above. The residual moisture (X_{RM}) ranges below 0.01 g·g^{-1} for most of the filter cakes. Performance differences between the six different container positions cannot be identified for the different containers with the oscillating temperature profile. The only outliers are the last filter cakes for the linear and progressive profile. Here, the residual moisture increases for container 4 and 5 for the progressive profile and for container 6 for the linear profile. For container 6 of the progressive profile, no predeliquored filter cake was obtainable in each of the three experiments due to clogging in the filtration module. The mother liquor could no longer be separated from the solid phase in the product suspension. The relatively high supersaturation at the end of the progressive profile led to crystal formation in the filtration module and filtrate tubing. A more detailed and figurative elaboration on this can be found in Chapter 6 of the Supporting Information.

From these observations, consequences for the long-term operation of the plant were drawn, as described in the following chapter.

3.3. Long-Term Experiments

From the findings of the quasi-continuous experiments with six consecutive containers, the operation strategy was developed for the long-term experiments. To avoid the clogging of the filtration module and a subsequent downtime of the plant, every fifth container was not filled with process medium. Whenever the empty container reaches the last module on the plant, water is introduced via the nozzles instead of ethanol, as it is performed for the washing step. For this rinsing step, water is sprayed for 30 min with an unchanged flow rate, which causes the dissolution of sucrose buildup in the module and piping, resulting in a clean filtration module. Besides this, the process parameters are kept the same as they have been for the previous experiments with the oscillating profile. The oscillating profile was selected due to the relatively high yield, the large product crystals, and the lowest deviations of the temperature profile. Relevant online measured process parameters (T and p) and offline measured quantities (Y_{FC} and X_{RM}) are demonstrated in Figure 11.

In panel (a), the suspension temperature of the containers on each module are plotted, demonstrating that, from the temperature control side, the long-term operation is feasible. The profiles are uniform and no major deviation can be seen. The integration of the rinsing step did not pose any challenges and the profiles were operated close to the target temperature.

In panel (b), the pressure in the filtration/washing/drying module is plotted. From the different pressure levels, one can clearly differentiate between the different integrated unit operations. The first pressure increase on each cycle is the filtration, which causes the initial separation between the filter cake and the filtrate. After the filter cake is predeliquored, the pressure decreases as air passes the filter cake. The filtration is followed by the filter cake washing for 20 s each cycle, where the ethanol is introduced as a washing liquid to the filter cake by the nozzles installed in the lid. For the rest of t_{cycle}, the filter cake is dried with heated air from the pressurized air network. After every fourth container, the filtration module, in particular the filter support and the filter pan, is rinsed with water under ambient pressure.

In panel (c), the PSDs of the product and the seed crystals are plotted as boxplots over time. The sample that has been taken for the analysis of the seed crystals belong to the same container, from which the product crystals come from that are plotted 2 h later in the diagram. Generally, uniform product particle properties can be observed across the 20 containers and 14 h of operation on the plant. Crystal growth and product PSDs are in the same range as they have been in the quasi-continuous experiments with six consecutive containers. Wider seed PSDs tend to also yield wider product PSDs.

Panel (d) of Figure 11 shows the relative yield Y_{FC} and X_{RM} determined after filtration, washing, and drying on the plant via the common loss on mass method described earlier. The residual moisture is on a low level of below 5 mg·g^{-1} for all filter cakes and substantially lower for most of them. A systematic effect on the deviations was not elaborated; however, the filter cakes that have been produced just before the rinsing step tend to have a higher X_{RM}, which can be explained by the more inefficient filtration due to the deposition

of sucrose in the filtration module. In terms of the Y_{FC}, the values increase over the time of 14 h, which can be explained by the evaporation of water from the stirred and heated storage vessel that contains the mother liquor used for the experiment. This has not been accounted for in the calculations at this point, but must be considered in future investigations. The yield Y_{FC} is also in the same range as it has been for previous experiments with little deviations.

In general, there was no indication that continuous operation beyond 14 h would fail. This period was the longest possible in the form of an extended laboratory day. An image of the received product filter cakes can be found in Supporting Material Figure S7.

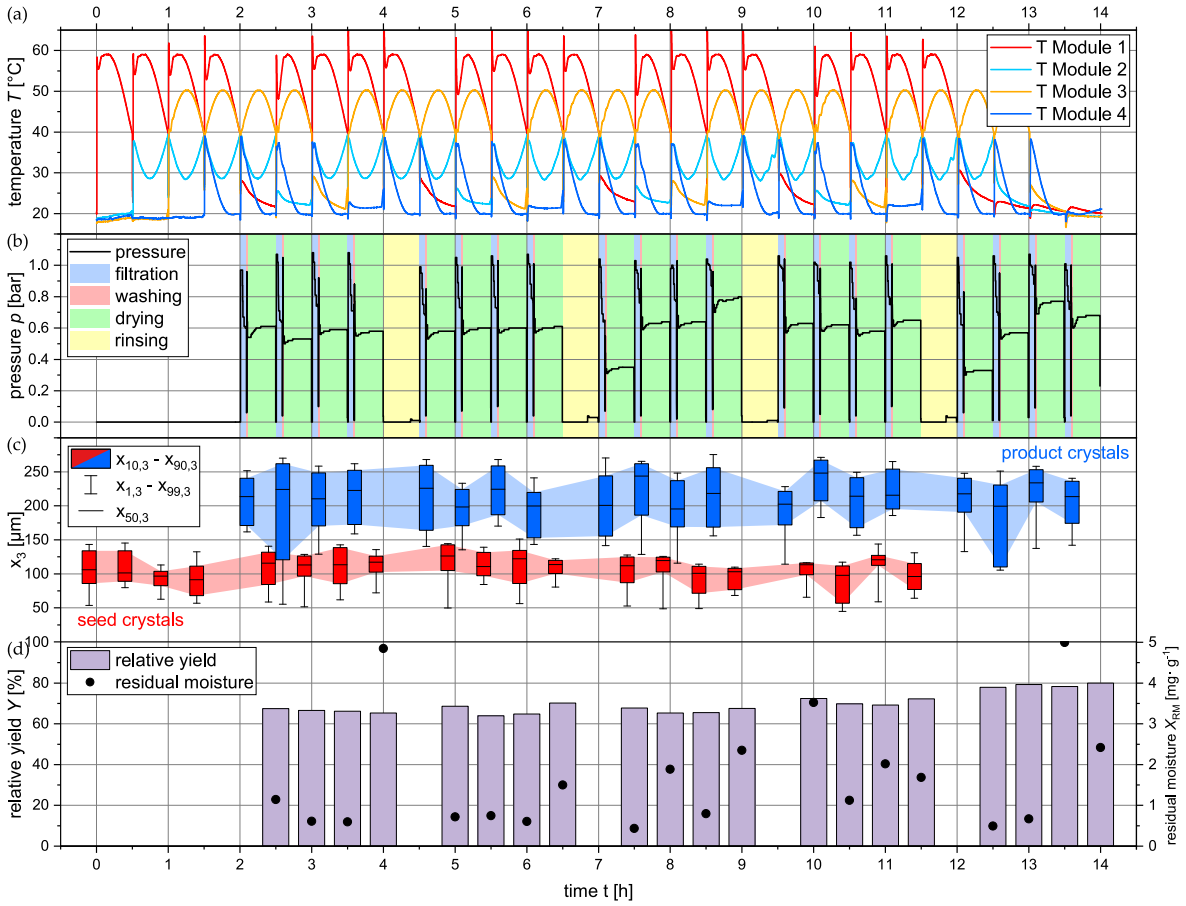

Figure 11. Panel plot of relevant processes and product parameters of the long-term operation of the QCFBC with 20 consecutive containers in total. In (**a**), the temperature curve of the four temperature modules is plotted according to the previously used color code. In (**b**), the pressure inside the container positioned on the last module is plotted. The unit operations filtration, washing, and drying as well as the rinsing step can be distinguished by the background colors. (**c**) shows the PSD for the seed crystals in red and the product crystals, collected right before the filtration, in blue. In panel (**d**), the relative yield calculated via the filter cake mass and the residual moisture of each of the product filter cake is plotted.

4. Conclusions

The quasi-continuous filter belt crystallizer QCFBC [57] was enlarged by a filtration, washing, and drying unit. The operation principle from [56,68] of the entire plant modeled in [63] has been further developed and long-term tested in this work. Based on the experiences described in [57], the modules for (positive pressure) filtration and filter cake washing were facilitated by the nozzles, and temperature-controlled convection drying has been individually designed, integrated into the existing setup, and characterized with idealized experimental conditions. This way is a suitable operation parameter for the quasi-continuous operation

for each of the unit operations which were elaborated using six consecutive containers. The proposed temperature profiles, needed for the previously characterized cooling crystallization [57], have been modified to work for the quasi-continuous operation principle with continuation on four subsequent temperature modules. This led to yields that were lower as they have been presented in [57]. Temperature deviations in the suspension caused by the switch between the modules added to this effect.

The model substance system sucrose/water now undergoes cooling crystallization, solid–liquid separation, filter cake washing, and convection drying on a single apparatus, resulting in a process chain that produces a dry filter cake at the end of the apparatus, starting with only seeded mother liquor. The implementation of positive pressure filtration also enabled for convection drying with temperature-controlled air and therefore high potential for filter cake drying. Overall uniform critical product quality attributes regarding residual moisture, product particle size, and relative yield ($x_{50,3}$ = 216.095 ± 14.766, $Y_{rel.}$ = 69.9% ± 5%, X_{RM} = 1.64 mg·g^{-1} ± 1.38 mg·g^{-1}) have been achieved. As actual small scale, the continuous production of particles as an integrated process is scarce, and the upgraded concept and plant are an attractive contribution featuring long-term operability.

It was successfully demonstrated that an automated and quasi-continuous long-term operation is possible without any disturbances or interruption for 14 h by including a rinsing cycle that clears out the filter pan resulting in a production of 15.026 g ± 1.151 g per container. Across the full operation of the plant, considering the full operation time of 14 h including the "startup" where no filter cake can be collected for the first 2.5 h, a production rate of 22.64 g·h^{-1} ± 1.64 g·h^{-1} was achieved. The last manual steps only include the seeding (solid handling is challenging, especially for small amounts), dosing of mother liquor (only for insights in the process), and the collection of the filter cake.

5. Outlook

Regarding the automation of the demonstrated setup, the last steps that need to be automated for a fully automated process are the container handling when it is not on the plant, the seeding, and the filter cake collection. The dosing of solid seed crystals is challenging due to the low amount of seed crystals needed for each container. However, a segmented dosing mechanism with previously filled individual sample carrier may be purposeful, since continuously delivering systems tend to clog. The second secondart that can be further automated is the removal of the filter cake that could simply be achieved by a product chute. For the removal of the container, a mechanical solution would be necessary.

Together with the temperature sensor, process analytical technology could (possibly optical or acoustical) be integrated in the lid to analyze the crystal suspension for online or inline control of the product quality and the process progress. The filtration, washing, and drying module is equipped with temperature sensors and a pressure sensor. It would be conceivable to implement an air mass flow sensor right before HE105 and a relative humidity sensor right after the air exits the filter cake to track the water content that is carried from the filter cakes. This way, online insights into the drying progress could be obtained, possibly saving energy since the drying can be stopped when product requirements are reached.

Integrating unit operations into the quasi-continuous operation principle of the plant highly benefits from the knowledge that has already been generated in batch operation. In addition, it was shown that it is possible to individually investigate the behavior of the already integrated unit operations, enabling for faster process development on two different levels. Firstly, further unit operations such as solid mixing, granulation, or compacting can be easily characterized and integrated into the plant, contributing to the targeted end-to-end production line, as presented by Domokos et al. [45]. Here, an end-to-end, continuous, and integrated production process of acetylsalicylic acid starting with an MSMPR coupled to the CFC with subsequent blending and tableting was presented.Secondly, faster introduction of new substance systems to the plant can be realized with easy adaption of substance-specific process parameters and the investigation of their respective influences. This, as well as

developing a general method for the introduction of new substance systems, are part of current work which should and will be investigated further.

For the selection of new substance systems, several points should be considered. Firstly, the substance should be soluble in water for the current setup. Special safety considerations such as explosion protection of occupational safety have not been undertaken so far. Secondly, the solubility should be highly temperature-dependent in the solvent. For a proper cake filtration, a filter cake needs to be formed. Additionally, especially in the context of current resource scarcity, mother liquor recycling should be implemented, enabling the reuse of the saturated filtrate.

Finally, three different levels of scale up of the plant can be investigated. Firstly, for simple linear scale up, the process volume in the container can be increased by up to 100%. Secondly, the amount of modules can simply be increased due to the modular concept. Neither modifications influence the dimensions of the container but can still lead to increased production rates. Thirdly, the complete plant, together with the modules and process medium compartments, can be up-scaled as it has been performed in [62], leading to a bigger plant footprint with considerably higher process medium volumes.

Supplementary Materials: The following supporting information can be downloaded at: https://www.mdpi.com/article/10.3390/pr11082457/s1, Figure S1. Image of the complete plant. The relevant periphery is indicated. Note that here the direction of operation is from right to left. Throughout the rest of this contribution, the operation is consistently demonstrated from left to right; Figure S2. In (a), the P&ID of the heater of the drying air is shown. This can also be found in the complete P&ID. In (b), the corresponding CAD sketch is shown. The heating element is colored in dark gray, while the 3D-printed parts are colored in beige. In (c), an image of the actual heat exchanger is shown; Figure S3. Setup of the container on the scale for continuous measurements of the residual moisture. The 3D-printed frame (ABS) enables for placing module and container on the scale at the same time; Figure S4. Image of the washing lid with the nozzles from below (a). The spray is turned on and slightly visible. In (b), the setup for the collection of the washing water can be seen; Figure S5. Concentration of the mother liquor during the oscillating temperature profile (small diagram) from experiments that have been performed solely for this purpose. The experimental conditions have been described elsewhere. The concentrations have been determined via the gravimetric method. Standard deviations in x- and y-direction stem from triple experiments. As before, the saturation line is from [65]; Figure S6. One exemplary pressure curve of the filtration, washing, and drying of 6 consecutive filter cakes after the progressive temperature profile. Images show the filter support from below, before, and after the 6 container campaigns; Figure S7. Image of the received product filter cakes from the long-term operation (14 h) of the complete plant; Video S1: Container and Container lid movement for after each t_{cycle}; Video S2: Schematic of the setup and operation principle of the QCFBC.

Author Contributions: Conceptualization, S.H.; methodology, S.H.; software, T.S. and S.H.; formal analysis, T.S. and S.H.; investigation, T.S., M.P., H.L. and S.H.; data curation, S.H.; writing—original draft preparation, S.H.; writing—review and editing, S.H. and N.K.; visualization, S.H.; supervision, S.H. and N.K.; project administration, N.K.; funding acquisition, N.K. All authors have read and agreed to the published version of the manuscript.

Funding: This research was funded by the German Federal Ministry of Economic Affairs and Climate Action (BMWK) and the Project Management Jülich (PtJ) as part of the ENPRO2.0 initiative (Ref. no. 03ET1652F). We acknowledge financial support by Deutsche Forschungsgemeinschaft and Technische Universität Dortmund/TU Dortmund University within the funding programme Open Access Costs.

Data Availability Statement: Not applicable.

Acknowledgments: The authors would like to thank Carsten Schrömges for technical support.

Conflicts of Interest: The authors declare no conflict of interest.

Abbreviations

The following abbreviations are used in this manuscript (also see Table 1):

ABS	Acrylonitrile butadiene styrene (for 3D printing)
API	Active pharmaceutical ingedient
ATC	Archimedes tube crystallizer
CCFD	Continuous carousel filter dryer
CFIC	Coiled flow inverter crystallizer
COBC	Continuous oscillatory baffle crystallizer
CRPF	Continuous rotary plate filter
CVSF	Continuous vacuum screw filter
DTB	Draft tube baffle crystallizer
ECM	Excess crystal mass
FC	Filter cake
GMP	Good manufacturing practice
ML	Mother liquor
MSMPR	Mixed suspension mixed product removal
P&ID	Piping and instrumentation diagram
PSD	Particle size distribution
PTFE	Polytetrafluoroethylene
QCFBC	Quasi-continuous filter belt crystallizer
RT	Residence time
RTD	Residence time distribution
SFC	Slug flow crystallizer
Dimensionless Numbers	
Re	Reynolds number (-)
Latin Symbols	
$c_{\text{suc.,wash,i}}$	Concentration of sucrose in wash medium ($g \cdot mL^{-1}$)
$c_{\text{tracer,i}}$	Concentration of tracer in wash medium ($g \cdot mL^{-1}$)
c^*	Saturation concentration ($g_{\text{succ}} \cdot g_{\text{sol}}^{-1}$)
ECM_{max}	Maximal excess crystal mass (g)
m_{FC}	Filter cake mass (g)
$m_{\text{FC,dry}}$	Dry filter cake mass (g)
$m_{\text{FC,max}}$	Maximal filter cake mass (g)
m_{SC}	Seed crystal mass (g)
m_{solid}	Mass of particles in FC (g)
$m_{\text{suc.,ML,0}}$	Mass of dissolved sucrose remaining in FC pores (g)
$m_{\text{suc.,wash,i}}$	Mass of sucrose washed from the filter cake (g)
m_{X}	Mass of remaining contaminant (g)
m_{ML}	Mass of mother liquor (g)
p	Pressure (bar)
T_{end}	Temperature at the end of the process (°C)
T_{start}	Temperature at the start of the process (°C)
$t_{\text{tot.}}$	total time of each container on the QCFBC (g)
V_{wash}	Volume of pores in FC (mL)
W	Wash ratio (-)
$x_{\text{aq.}}$	Water content in mL ($g \cdot g^{-1}$)
X_{RM}	Residual moisture ($g \cdot g^{-1}$)
X^*_{end}	Saturation loading at the end of the crystallization ($g \cdot g^{-1}$)
X^*_{start}	Saturation loading at the start of the crystallization ($g \cdot g^{-1}$)
X^*	Contaminant loading in FC ($g \cdot g^{-1}$)
$Y_{\text{filtrate,rel.}}$	Relative yield derived from the filtrate concentration (-)
$Y_{\text{FC,rel.}}$	Relative yield derived from the filter cake (-)
Greek Symbols	
ΔX_{RM}	Change in residual moisture ($g \cdot g^{-1}$)
$\rho(x)$	Density depending on the composition ($kg \cdot L^{-1}$)
ϑ	Temperature (°C)

References

1. Myerson, A.S. (Ed.) *Handbook of Industrial Crystallization*, 2nd ed.; Elsevier: Amsterdam, The Netherlands, 2002. [CrossRef]
2. Hofmann, G. (Ed.) *Kristallisation in der Industriellen Praxis*; Wiley: Hoboken, NJ, USA, 2004. [CrossRef]
3. am Ende, D.J.; am Ende, M.T., Eds. *Chemical Engineering in the Pharmaceutical Industry*; Wiley: Hoboken, NJ, USA, 2019. [CrossRef]
4. Beckmann, W. *Crystallization: Basic Concepts and Industrial Applications*; Wiley: Hoboken, NJ, USA, 2013. [CrossRef]
5. Khinast, J.; Rantanen, J. *Continuous Manufacturing of Pharmaceuticals*; Wiley: Hoboken, NJ, USA, 2017. [CrossRef]
6. Wood, B.; Girard, K.P.; Polster, C.S.; Croker, D.M. Progress to Date in the Design and Operation of Continuous Crystallization Processes for Pharmaceutical Applications. *Org. Process. Res. Dev.* **2019**, *23*, 122–144. [CrossRef]
7. Acevedo, D.; Peña, R.; Yang, Y.; Barton, A.; Firth, P.; Nagy, Z.K. Evaluation of mixed suspension mixed product removal crystallization processes coupled with a continuous filtration system. *Chem. Eng. Process. Process. Intensif.* **2016**, *108*, 212–219. [CrossRef]
8. Chen, J.; Sarma, B.; Evans, J.M.; Myerson, A.S. Pharmaceutical crystallization. *Cryst. Growth Des.* **2011**, *11*, 887–895. [CrossRef]
9. Kreimer, M.; Aigner, I.; Lepek, D.; Khinast, J. Continuous Drying of Pharmaceutical Powders Using a Twin-Screw Extruder. *Org. Process. Res. Dev.* **2018**, *22*, 813–823. [CrossRef]
10. Bieringer, T.; Buchholz, S.; Kockmann, N. Future Production Concepts in the Chemical Industry: Modular— Small-Scale—Continuous. *Chem. Eng. Technol.* **2013**, *36*, 900–910. [CrossRef]
11. Cote, A.; Erdemir, D.; Girard, K.P.; Green, D.A.; Lovette, M.A.; Sirota, E.; Nere, N.K. Perspectives on the Current State, Challenges, and Opportunities in Pharmaceutical Crystallization Process Development. *Cryst. Growth Des.* **2020**, *20*, 7568–7581. [CrossRef]
12. Zhang, D.; Xu, S.; Du, S.; Wang, J.; Gong, J. Progress of Pharmaceutical Continuous Crystallization. *Engineering* **2017**, *3*, 354–364. [CrossRef]
13. Kurt, S.K.; Akhtar, M.; Nigam, K.D.P.; Kockmann, N. Continuous Reactive Precipitation in a Coiled Flow Inverter: Inert Particle Tracking, Modular Design, and Production of Uniform CaCO3 Particles. *Ind. Eng. Chem. Res.* **2017**, *56*, 11320–11335. [CrossRef]
14. Lee, S.L.; O'Connor, T.F.; Yang, X.; Cruz, C.N.; Chatterjee, S.; Madurawe, R.D.; Moore, C.M.; Yu, L.X.; Woodcock, J. Modernizing Pharmaceutical Manufacturing: From Batch to Continuous Production. *J. Pharm. Innov.* **2015**, *10*, 191–199. [CrossRef]
15. Ma, Y.; Wu, S.; Macaringue, E.G.J.; Zhang, T.; Gong, J.; Wang, J. Recent Progress in Continuous Crystallization of Pharmaceutical Products: Precise Preparation and Control. *Org. Process. Res. Dev.* **2020**, *24*, 1785–1801. [CrossRef]
16. Mascia, S.; Heider, P.L.; Zhang, H.; Lakerveld, R.; Benyahia, B.; Barton, P.I.; Braatz, R.D.; Cooney, C.L.; Evans, J.M.; Jamison, T.F.; et al. End-to-end continuous manufacturing of pharmaceuticals: Integrated synthesis, purification, and final dosage formation. *Angew. Chem. Int. Ed.* **2013**, *52*, 12359–12363. [CrossRef]
17. Seifert, T.; Sievers, S.; Bramsiepe, C.; Schembecker, G. Small scale, modular and continuous: A new approach in plant design. *Chem. Eng. Process. Process. Intensif.* **2012**, *52*, 140–150. [CrossRef]
18. Lier, S.; Paul, S.; Ferdinand, D.; Grünewald, M. Modulare Verfahrenstechnik: Apparateentwicklung für wandlungsfähige Produktionssysteme. *Chemie-Ingenieur-Technik* **2016**, *88*, 1444–1454. . [CrossRef]
19. Wang, T.; Lu, H.; Wang, J.; Xiao, Y.; Zhou, Y.; Bao, Y.; Hao, H. Recent progress of continuous crystallization. *J. Ind. Eng. Chem.* **2017**, *54*, 14–29. [CrossRef]
20. Orehek, J.; Teslić, D.; Likozar, B. Continuous Crystallization Processes in Pharmaceutical Manufacturing: A Review. *Org. Process. Res. Dev.* **2021**, *25*, 16–42. [CrossRef]
21. Chianese, A.; Kramer, H.J. *Industrial Crystallization Process Monitoring and Control*; Wiley: Hoboken, NJ, USA, 2012. [CrossRef]
22. Lier, S.; Wörsdörfer, D.; Grünewald, M. Transformable Production Concepts: Flexible, Mobile, Decentralized, Modular, Fast. *Chemie-Ingenieur-Technik* **2015**, *87*, 1147–1158. [CrossRef]
23. Domokos, A.; Nagy, B.; Szilágyi, B.; Marosi, G.; Nagy, Z.K. Integrated Continuous Pharmaceutical Technologies—A Review. *Org. Process. Res. Dev.* **2021**, *25*, 721–739. [CrossRef]
24. Hohmann, L.; Gorny, R.; Klaas, O.; Ahlert, J.; Wohlgemuth, K.; Kockmann, N. Design of a Continuous Tubular Cooling Crystallizer for Process Development on Lab-Scale. *Chem. Eng. Technol.* **2016**, *39*, 1268–1280. [CrossRef]
25. Hohmann, L.; Schmalenberg, M.; Prasanna, M.; Matuschek, M.; Kockmann, N. Suspension flow behavior and particle residence time distribution in helical tube devices. *Chem. Eng. J.* **2019**, *360*, 1371–1389. [CrossRef]
26. Hohmann, L.; Greinert, T.; Mierka, O.; Turek, S.; Schembecker, G.; Bayraktar, E.; Wohlgemuth, K.; Kockmann, N. Analysis of Crystal Size Dispersion Effects in a Continuous Coiled Tubular Crystallizer: Experiments and Modeling. *Cryst. Growth Des.* **2018**, *18*, 1459–1473. [CrossRef]
27. Termühlen, M.; Strakeljahn, B.; Schembecker, G.; Wohlgemuth, K. Characterization of slug formation towards the performance of air-liquid segmented flow. *Chem. Eng. Sci.* **2019**, *207*, 1288–1298. [CrossRef]
28. Termühlen, M.; Etmanski, M.M.; Kryschewski, I.; Kufner, A.C.; Schembecker, G.; Wohlgemuth, K. Continuous slug flow crystallization: Impact of design and operating parameters on product quality. *Chem. Eng. Res. Des.* **2021**, *170*, 290–303. [CrossRef]
29. Termühlen, M.; Strakeljahn, B.; Schembecker, G.; Wohlgemuth, K. Quantification and evaluation of operating parameters' effect on suspension behavior for slug flow crystallization. *Chem. Eng. Sci.* **2021**, *243*, 116771. [CrossRef]
30. Steenweg, C.; Kufner, A.; Habicht, J.; Wohlgemuth, K. Towards continuous primary manufacturing processes—Particle design through combined crystallization and particle isolation. *Processes* **2021**, *9*, 2187. [CrossRef]

31. Sonnenschein, J.; Wohlgemuth, K. Archimedes tube crystallizer: Design and characterization for small-scale continuous crystallization. *Chem. Eng. Res. Des.* **2022**, *178*, 488–501. [CrossRef]
32. Sonnenschein, J.; Heming, R.; Wohlgemuth, K. Archimedes Tube Crystallizer: Design and Operation of Continuous Cooling Crystallization Based on First-Principle Modeling. *Cryst. Growth Des.* **2022**, *22*, 5272–5284. [CrossRef]
33. Ottoboni, S.; Price, C.J.; Steven, C.; Meehan, E.; Barton, A.; Firth, P.; Mitchell, A.; Tahir, F. Development of a Novel Continuous Filtration Unit for Pharmaceutical Process Development and Manufacturing. *J. Pharm. Sci.* **2019**, *108*, 372–381. [CrossRef]
34. NiTech Solutions Continuous Processing Reactors and Crystallisers. Available online: https://www.nitechsolutions.co.uk/ (accessed on 14 April 2023).
35. Kacker, R.; Regensburg, S.I.; Kramer, H.J.M. Residence time distribution of dispersed liquid and solid phase in a continuous oscillatory flow baffled crystallizer. *Chem. Eng. J.* **2017**, *317*, 413–423. [CrossRef]
36. Vetter, T.; Burcham, C.L.; Doherty, M.F. Regions of attainable particle sizes in continuous and batch crystallization processes. *Chem. Eng. Sci.* **2014**, *106*, 167–180. [CrossRef]
37. Schmalenberg, M.; Nocon, A.K.; Kockmann, N. Design and Hydrodynamic Characterization of a Draft Tube Baffle Tank for Lab-Scale. *Chem. Ing. Tech.* **2020**, *92*, 288–294. [CrossRef]
38. Schmalenberg, M.; Krell, T.; Mathias, C.; Kockmann, N. Continuous Miniaturized Draft Tube Baffle Crystallizer with Particle Screw for Supportive Suspension Discharge. *Ind. Eng. Chem. Res.* **2021**, *60*, 18094–18105. [CrossRef]
39. Schmalenberg, M.; Mensing, L.; Lindemann, S.; Krell, T.; Kockmann, N. Miniaturized draft tube baffle crystallizer for continuous cooling crystallization. *Chem. Eng. Res. Des.* **2022**, *178*, 232–250. [CrossRef]
40. Caldwell, H.B. Modern Concepts of Crystallization. *Ind. Eng. Chem.* **1961**, *53*, 115–118. [CrossRef]
41. Barton, A.W. *WO 2015/033117 A1;* Filtration Apparatus. 12 March 2015.
42. Ottoboni, S.; Coleman, S.J.; Steven, C.; Siddique, M.; Fraissinet, M.; Joannes, M.; Laux, A.; Barton, A.; Firth, P.; Price, C.J.; et al. Understanding API static drying with hot gas flow: Design and test of a drying rig prototype and drying modeling development. *Org. Process. Res. Dev.* **2020**, *24*, 2505–2520. [CrossRef]
43. Ottoboni, S.; Shahid, M.; Steven, C.; Coleman, S.; Meehan, E.; Barton, A.; Firth, P.; Sutherland, R.; Price, C.J. Developing a Batch Isolation Procedure and Running It in an Automated Semicontinuous Unit: AWL CFD25 Case Study. *Org. Process. Res. Dev.* **2020**, *24*, 520–539. [CrossRef] [PubMed]
44. Nagy, B.; Szilágyi, B.; Domokos, A.; Tacsi, K.; Pataki, H.; Marosi, G.; Nagy, Z.K.; Nagy, Z.K. Modeling of pharmaceutical filtration and continuous integrated crystallization-filtration processes. *Chem. Eng. J.* **2021**, *413*, 127566. [CrossRef]
45. Domokos, A.; Nagy, B.; Gyürkés, M.; Farkas, A.; Tacsi, K.; Pataki, H.; Liu, Y.C.; Balogh, A.; Firth, P.; Szilágyi, B.; et al. End-to-end continuous manufacturing of conventional compressed tablets: From flow synthesis to tableting through integrated crystallization and filtration. *Int. J. Pharm.* **2020**, *581*. [CrossRef] [PubMed]
46. Liu, Y.C.; Domokos, A.; Coleman, S.; Firth, P.; Nagy, Z.K. Development of Continuous Filtration in a Novel Continuous Filtration Carousel Integrated with Continuous Crystallization. *Org. Process. Res. Dev.* **2019**, *23*, 2655–2665. [CrossRef]
47. Destro, F.; Hur, I.; Wang, V.; Abdi, M.; Feng, X.; Wood, E.; Coleman, S.; Firth, P.; Barton, A.; Barolo, M.; et al. Mathematical modeling and digital design of an intensified filtration-washing-drying unit for pharmaceutical continuous manufacturing. *Chem. Eng. Sci.* **2021**, *244*, 116803. [CrossRef]
48. Destro, F.; Nagy, Z.K.; Barolo, M. A benchmark simulator for quality-by-design and quality-by-control studies in continuous pharmaceutical manufacturing – Intensified filtration-drying of crystallization slurries. *Comput. Chem. Eng.* **2022**, *163*, 107809. [CrossRef]
49. Destro, F.; Barolo, M.; Nagy, Z.K. Quality-by-control of intensified continuous filtration-drying of active pharmaceutical ingredients. *AIChE J.* **2023**, *69*, e17926. [CrossRef]
50. Testa, C.J.; Hu, C.; Shvedova, K.; Wu, W.; Sayin, R.; Casati, F.; Halkude, B.S.; Hermant, P.; Shen, D.E.; Ramnath, A.; et al. Design and Commercialization of an End-to-End Continuous Pharmaceutical Production Process: A Pilot Plant Case Study. *Org. Process. Res. Dev.* **2020**, *24*, 2874–2889. [CrossRef]
51. Testa, C.J.; Shvedova, K.; Hu, C.; Wu, W.; Born, S.C.; Takizawa, B.; Mascia, S. Heterogeneous Crystallization as a Process Intensification Technology in an Integrated Continuous Manufacturing Process for Pharmaceuticals. *Org. Process. Res. Dev.* **2021**, *25*, 225–238. [CrossRef]
52. Hu, C.; Testa, C.J.; Born, S.C.; Wu, W.; Shvedova, K.; Sayin, R.; Halkude, B.S.; Casati, F.; Ramnath, A.; Hermant, P.; et al. E-factor analysis of a pilot plant for end-to-end integrated continuous manufacturing (ICM) of pharmaceuticals. *Green Chem.* **2020**, *22*, 4350–4356. [CrossRef]
53. Schembecker, G.; Wohlgemuth, K.; Steenweg, C.M. *WO 2021/148108 A1;* Rotating-Screw Drying Reactor. 6 May 2023.
54. Steenweg, C.; Seifert, A.; Wohlgemuth, K.; Schembecker, G. Characterization of a modular continuous vacuum screw filter for small-scale solid–liquid separation of suspensions. *ACS Publ.* **2021**, *25*, 940. [CrossRef]
55. Steenweg, C.; Seifert, A.I.; Böttger, N.; Wohlgemuth, K. Process Intensification Enabling Continuous Manufacturing Processes Using Modular Continuous Vacuum Screw Filter. *Org. Process. Res. Dev.* **2021**, *25*, 2525–2536. [CrossRef]
56. Dobler, T.; Buchheiser, S.; Gleiß, M.; Nirschl, H. Development and Commissioning of a Small-Scale, Modular and Integrated Plant for the Quasi-Continuous Production of Crystalline Particles. *Processes* **2021**, *9*, 663. [CrossRef]
57. Höving, S.; Oldach, B.; Kockmann, N. Cooling Crystallization with Complex Temperature Profiles on a Quasi-Continuous and Modular Plant. *Processes* **2022**, *10*, 1047. [CrossRef]

58. Thurner, F. Der Titus-Nutsch-Trockner – Neue Wege der Produktisolierung. *Chem. Ing. Tech.* **1990**, *62*, 753–755. [CrossRef]
59. Schweigler, N.; Gehrmann, D.; Bamberger, T.; Tichy, J. Kontinuierliche Filtration und Trocknung auf einem neuartigen Filtertrockner (Konfiltro). *Chem. Ing. Tech.* **1995**, *67*, 1186–1187. [CrossRef]
60. Kockmann, N. Modular Equipment for Chemical Process Development and Small-Scale Production in Multipurpose Plants. *Chembioeng Rev.* **2016**, *3*, 5–15. [CrossRef]
61. Höving, S.; Bolien, P.; Siebers, P.; Kockmann, N. Simplified Approach to Characterize the Cooling Crystallization in a Modular Mini-Plant. *Crystals* **2023**, *13*, 147. [CrossRef]
62. Dobler, T.; Höving, S.; Dreiser, C.; Gleiß, M.; Gröschen, M.; Henkel, A.; Hörne, M.; Schäfer, M.; Sonnenschein, J.; Wiese, G.; et al. From Lab to Pilot Scale: Commissioning of an Integrated Device for the Generation of Crystals. *Chem. Eng. Technol.* **2023**. [CrossRef]
63. Sonnenschein, J.; Hermes, M.; Höving, S.; Kockmann, N.; Wohlgemuth, K. Population balance modeling of unstirred cooling crystallization on an integrated belt filter. *Comput. Chem. Eng.* **2022**, *167*, 108024. [CrossRef]
64. Höving, S.; Neuendorf, L.; Betting, T.; Kockmann, N. Determination of Particle Size Distributions of Bulk Samples Using Micro-Computed Tomography and Artificial Intelligence. *Materials* **2023**, *16*, 1002. [CrossRef]
65. Wilson, A.J.C. Atlas der Zuckerkristalle—Atlas of Sugar Crystals by G. Vavrinecz. *Acta Crystallogr.* **1966**, *20*. [CrossRef]
66. Schneider, F.; Schliephake, D. Dichtetabelle für wässrige Saccharoselösungen. *Sonderbeil. Zur Z. Zucker* **1963**, *10*, 1–19.
67. Bretschneider, R.; Kadlec, P.; Dandâr, A.; Bubnik, Z. Dichte von Zuckerlösungen. *Zuckerindustrie* **1979**, *104*, 719–722.
68. L̀obnitz, L. Auslegung des Separationsprozesses und Entwicklung neuer Verfahrenskonzepte zur integrierten Produktion und Separation kristalliner Aminos̀auren. Ph.D. Thesis, Karlsruher Institut f̀ur Technologie (KIT), Karlsruhe, Germany, 2020.
69. Schneider, F. (Ed.) *Sugar Analysis: Official and Tentative Methods Recommended by the International Commission for Uniform Methods of Sugar Analysis (ICUMSA)*; ICUMSA: Boronia Heights, Australia, 1979 .
70. Schneider, F.; Schliephake, D.; Klimmek, A. Über die Viscosität von reinen Saccharoselösungen. *Zuckerindustrie* **1963**, *16*, 465–473.
71. Dobler, T.; Radel, B.; Gleiss, M.; Nirschl, H. Quasi-Continuous Production and Separation of Lysozyme Crystals on an Integrated Laboratory Plant. *Crystals* **2021**, *11*, 713. [CrossRef]
72. Pot, A. Industrial Sucrose Crystallisation: A Study on the Development of Crystal Size Distributions in Continuous and Batch Sucrose Suspension Crystallisers. Ph.D. Thesis, TU Delft, Delft, The Netherlands, 1983.
73. Bouchard, A.; Hofland, G.W.; Witkamp, G.J. Properties of Sugar, Polyol, and Polysaccharide Water-Ethanol Solutions. *J. Chem. Eng. Data* **2007**, *52*, 1838–1842. [CrossRef]
74. Ruslim, F.; Hoffner, B.; Nirschl, H.; Stahl, W. Evaluation of pathways for washing soluble solids. *Chem. Eng. Res. Des.* **2009**, *87*, 1075–1084. [CrossRef]
75. Brückner, A.; Sprott, T.; Peuker, U.A.; Hoffner, B. Influence of pre-dewatering on the success of cake washing. *Sep. Sci. Technol.* **2023**, *58*, 175–187. [CrossRef]